

1 **Title: Short-term social isolation acts on hypothalamic neurons to promote social**
2 **behavior in a sex- and context-dependent manner.**

3 Xin Zhao¹, Yurim Chae¹, Destiny Smith¹, Valerie Chen¹, Dylan DeFelipe¹, Joshua W Sokol¹,
4 Archana Sadangi¹, and Katherine Tschida¹

5 ¹Department of Psychology, Cornell University, Ithaca NY 14853

6 *Corresponding Author: Katherine Tschida, kat227@cornell.edu

7 **Abstract**

8 Social animals, including both humans and mice, are highly motivated to engage in
9 social interactions. Short-term social isolation increases social motivation and promotes
10 social behavior, but the neural circuits through which it does so remain incompletely
11 understood. Here, we sought to identify neurons that promote social behavior in single-
12 housed female mice, which exhibit increased rates of social investigation, social ultrasonic
13 vocalizations (USVs), and mounting during same-sex interactions that follow a period of
14 short-term (3-day) isolation. We first used immunostaining for the immediate early gene Fos
15 to identify a population of neurons in the preoptic hypothalamus (POA) that increase their
16 activity in single-housed females following same-sex interactions (POA_{iso} neurons). TRAP2-
17 mediated chemogenetic silencing of POA_{iso} neurons in single-housed females significantly
18 attenuates the effects of short-term isolation on social investigation and USV production and
19 also tends to reduce mounting. In contrast, caspase-mediated ablation of POA_{iso} neurons in
20 single-housed females robustly attenuates mounting but has no effect on social investigation
21 or USV production. Optogenetic activation of POA_{iso} neurons in group-housed females
22 promotes USV production but does not recapitulate the effects of short-term isolation on
23 social investigation and mounting. To understand whether a similar population of POA_{iso}
24 neurons promotes social behavior in single-housed males, we performed Fos
25 immunostaining in single-housed males following either same-sex or opposite-sex social
26 interactions. These experiments revealed a population of POA neurons that increase Fos
27 expression in single-housed males following opposite-sex, but not same-sex, interactions.
28 Chemogenetic silencing of POA_{iso} neurons in single-housed males during interactions with
29 females tends to reduce mounting but does not decrease social investigation or USV
30 production. These experiments identify a population of hypothalamic neurons that promote
31 social behavior following short-term isolation in a sex- and social context-dependent manner.

32 **Keywords:** social isolation, ultrasonic vocalization, preoptic hypothalamus, mounting,
33 female

34 **Introduction**

35 Humans and other social mammals find social interactions rewarding and are highly
36 motivated to seek out social connections. Consequently, the experience of social isolation is
37 aversive and impacts both our brains and our behaviors. While long-term isolation can lead
38 to the emergence of anti-social behaviors in both humans and rodents (An et al., 2017;
39 Arrigo and Bullock, 2008; Check et al., 1985; Hossain et al., 2020; Killgore et al., 2021; Ma
40 et al., 2011, 2022; Machimbarrena et al., 2019; Matsumoto et al., 2005; Mears and Bales,
41 2009; Reid et al., 2022; Toth et al., 2011; Valzelli, 1973; Weiss et al., 2004; Wiberg and
42 Grice, 1963; Zelikowsky et al., 2018), short-term isolation typically increases levels of social
43 motivation and promotes social-seeking behaviors (Baumeister and Leary, 1995; Cacioppo
44 et al., 2006; Cacioppo and Cacioppo, 2018; House et al., 1988; Lee et al., 2021; Niesink and
45 van Ree, 1982; Panksepp and Beatty, 1980; Zhao et al., 2021). Alterations in social
46 motivation are characteristic of many neurodevelopmental disorders, including autism
47 spectrum disorder (Chevallier et al., 2012; Clements et al., 2018). How short-term social
48 isolation acts on the brain to promote social behavior remains incompletely understood.

49 Mesolimbic circuits play an important role in regulating social motivation and social
50 reward, during courtship as well as during same-sex interactions (Bariselli et al., 2018; Dai et
51 al., 2022; Dölen et al., 2013; Gunaydin et al., 2014; Hung et al., 2017; Love, 2014; Melis et
52 al., 2022; Resendez et al., 2020; Robinson et al., 2011; Solié et al., 2022; Tang et al., 2014;
53 Walum and Young, 2018; Xiao et al., 2017). In line with their role in regulating social
54 behavior, changes in the function of mesolimbic circuits have been reported following long-
55 term (weeks-long) social isolation and/or early-life social isolation (McWain et al., 2022;
56 Musardo et al., 2022; Tan et al., 2021; Yorgason et al., 2016). The neural circuit changes
57 that mediate the effects of short-term isolation on social motivation in adult animals are
58 comparatively less explored, but here as well, recent studies in both humans and rodents
59 have implicated changes in various populations of midbrain dopamine neurons (Inagaki et
60 al., 2016; Matthews et al., 2016; Tomova et al., 2020). Beyond its effects on mesolimbic
61 circuits, whether social isolation acts on additional neuronal populations to promote social
62 interaction is unknown.

63 In recent work, we found that short-term (3-day) social isolation exerts robust effects
64 on the social behaviors of C57BL/6J female mice (Zhao et al., 2021). Relative to group-
65 housed females, single-housed females that subsequently engaged in same-sex interactions
66 exhibited increased rates of social investigation, increased rates of USVs, and were also
67 observed to mount female social partners, a behavior never observed in pairs of group-

68 housed females (Zhao et al., 2021). The robust effect of short-term isolation on these three
69 aspects of female social behavior provides a powerful paradigm to identify neurobiological
70 changes that mediate the effects of short-term isolation on social behavior. In the current
71 study, we combined this behavioral paradigm with Fos immunostaining and the TRAP2
72 activity-dependent labeling approach (Allen et al., 2017; DeNardo et al., 2019) to identify and
73 characterize a population of neurons in the preoptic hypothalamus that increase their activity
74 in single-housed females following same-sex social interactions (i.e., POA_{iso} neurons). We
75 next asked whether silencing or ablation of POA_{iso} neurons attenuates the effects of short-
76 term isolation on female social behavior, and whether artificial activation of POA_{iso} neurons
77 in group-housed females mimics the effects of short-term isolation on female social
78 behavior. Finally, we extended a subset of these experiments to single-housed males
79 engaged in opposite-sex and same-sex interactions, to understand whether short-term
80 isolation acts on the POA to promote social behavior in a manner that depends on either sex
81 or social context. This study identifies novel neurobiological mechanisms through which
82 short-term social isolation acts on the brain to promote social interaction. Our findings also
83 add to an emerging literature indicating that the POA regulates not only sexual behavior but
84 also female social behavior during same-sex interactions.

85 **Results**

86 **Neurons in the preoptic hypothalamus increase their activity in socially isolated** 87 **female mice following same-sex social interactions**

88 To identify changes in neuronal activity that may underlie the effects of short-term
89 isolation on female social behavior, we performed immunostaining for the immediate early
90 gene Fos in brain sections collected from group-housed and single-housed (3-days) subject
91 females following 30-minute social encounters in their home cages with a novel, group-
92 housed visitor female (Fig. 1A). In line with our previous behavioral findings (Zhao et al.,
93 2021), we observed that single-housed female residents spent more time investigating
94 visitors (Fig. 1B; Mann-Whitney U test, $p = 0.001$) and in many trials mounted visitors, a
95 behavior that was not observed in group-housed residents (Fig. 1C; 0 of 12 group-housed
96 residents and 10 of 13 single-housed residents mounted visitors; Mann-Whitney U test for
97 difference in total mounting duration, $p < 0.001$; see Table S1 for complete statistical
98 details). Female pairs that contained a single-housed resident also produced higher rates of
99 ultrasonic vocalizations (USVs) than pairs with a group-housed resident (Fig. 1D; Mann-
100 Whitney U test, $p < 0.001$). Although either female in a dyad can produce USVs (Warren et
101 al., 2020), the robust effects of short-term isolation on the non-vocal social behaviors of
102 single-housed females suggest that at least some of the elevation in USV rates is driven by

103 increased USV production by the single-housed resident. Given the robust effects of short-
104 term isolation on these three aspects of female social behavior, we focused our analyses on
105 two hypothalamic regions implicated in regulating these behaviors: the preoptic area (POA),
106 which regulates social approach (McHenry et al., 2017), social reward (Hu et al., 2021),
107 mounting (Floody, 1989; Karigo et al., 2021; Wei et al., 2018) and USV production (Chen et
108 al., 2021; Gao et al., 2019; Green et al., 2018; Karigo et al., 2021; Michael et al., 2020); and
109 the ventromedial hypothalamus (VMH), which regulates mounting (Hashikawa et al., 2017;
110 Karigo et al., 2021; Lee et al., 2014; Liu et al., 2022). We also examined Fos expression
111 within the caudolateral periaqueductal gray (PAG), based on the well-established role of this
112 region in the control of vocalization in vertebrates and USV production in mice (Chen et al.,
113 2021; Jürgens, 1994; Michael et al., 2020; Tschida et al., 2019). To test whether any
114 observed differences in Fos expression in these three regions were associated with
115 isolation-induced changes in social behavior rather than baseline differences between
116 groups, we also measured Fos expression in the POA, the VMH, and the PAG of group-
117 housed and single-housed females that did not engage in social interaction with novel
118 female visitors (Fig. 1E-F; Fig. S1).

119 These analyses revealed that baseline levels of Fos expression within the POA and
120 the VMH did not differ between group-housed and single-housed females (Fig. 1F, left and
121 middle, open bars; two-way ANOVA to analyze Fos expression within each brain region,
122 factor 1 = housing status, factor 2 = social interaction, followed by post-hoc Tukey's HSD
123 tests). Following social interactions with novel female visitors, single-housed females
124 exhibited robust increases in Fos expression within the POA (Fig. 1F, left; $p < 0.001$) but not
125 within the VMH (Fig. 1F, middle; $p > 0.05$). In contrast, Fos expression within these two brain
126 areas did not increase significantly in group-housed females that interacted with novel
127 female visitors (Fig. 1F; $p > 0.05$ for both comparisons). Similar to the POA, baseline Fos
128 expression within the PAG did not differ between group-housed and single-housed females
129 ($p > 0.05$), and only single-housed females displayed increased PAG Fos expression
130 following social interactions with novel female visitors (Fig. 1F, right; $p < 0.001$), a finding
131 that further supports the idea that single-housed females increase USV production during
132 same-sex interactions. POA Fos expression was significantly and positively correlated with
133 the total amount of time spent in resident-initiated investigation for both group-housed and
134 single-housed females (Fig. S1C, left; linear regression, $p < 0.05$), as well as with the total
135 number of mounting bouts produced by single-housed resident females (Fig. S1C, middle; p
136 < 0.01). In both group-housed and single-housed female residents, Fos expression tended
137 to correlate positively with total USVs, but these relationships were not significant (Fig. S1C,
138 right; $p > 0.05$ for both comparisons; see Fig. S1D-E for relationships of VMH Fos and PAG
139 Fos to vocal and non-vocal social behaviors). In summary, POA Fos expression increases

140 selectively in single-housed females following social interactions, and levels of POA Fos
141 expression are also well related to the production of specific types of social behaviors by
142 single-housed females.

143 To ask whether the effects of short-term isolation on female social behavior and POA
144 Fos expression are long-lasting, we measured social behaviors of female residents at three
145 timepoints: (1) on day 0, when female subjects were still group-housed; (2) on day 3, after
146 female subjects had been single-housed for 3 days; and (3) on day 17, after half of the
147 subject females had been re-group-housed with their same-sex siblings for two weeks and
148 the other half of the subject females remained single-housed for two weeks (Figs. 1G-I).
149 Brains of re-group-housed and 14-day single-housed subject females were collected after
150 the day 17 social interaction, and Fos expression within the POA was examined (Fig. 1K).
151 Consistent with our earlier findings, rates of social investigation and USV production
152 significantly increased following 3 days of social isolation (Fig. 1G, I; one-way ANOVAs with
153 repeated measures; $p < 0.05$ for day 0 vs. day 3 in both groups for both behaviors).
154 Following re-group-housing, time spent in social investigation and rates of USV production
155 tended to decrease to pre-isolation levels (Fig. 1G, I, top plots; $p = 0.06$ for day 0 vs. day 17
156 investigation time and day 0 vs. day 17 total USVs in re-group-housed females). In contrast,
157 females that were single-housed for 14 days continued to spend increased time in social
158 investigation (Fig. 1G, bottom plot; $p < 0.05$ for day 0 vs. day 3 investigation and for day 0
159 vs. day 17 investigation), and pairs containing 14-day single-housed residents continued to
160 produce elevated rates of USVs (Fig. 1I, bottom plot; $p < 0.05$ for day 0 vs. day 3 USVs and
161 for day 0 vs. day 17 USVs). Time spent mounting tended to follow the same trends as rates
162 of social investigation and USV production in re-group-housed and 14-day single-housed
163 females (Fig. 1H). Along with the attenuation of female social behaviors following re-group-
164 housing, we also found that POA Fos expression was significantly lower in re-group-housed
165 females relative to 14-day single-housed females (Fig. 1K; t-test, $p < 0.001$). These findings
166 support the idea that changes in female social behavior following short-term isolation are
167 reversible and are accompanied by decreased POA Fos expression. Hereinafter, we refer to
168 the population of POA neurons that increase Fos expression in single-housed females that
169 have engaged in same-sex interactions as POA_{iso} neurons, and we next conducted
170 experiments to test whether functional manipulations of POA_{iso} neuronal activity impact the
171 effects of short-term isolation on female social behavior.

172 **Chemogenetic inhibition of POA_{iso} neurons attenuates the effects of social isolation** 173 **on female social investigation and USV production**

174 If increased activity of POA_{iso} neurons contributes to the effects of short-term
175 isolation on female social behavior, one prediction is that reducing the activity of POA_{iso}

176 neurons in single-housed females will attenuate the effects of isolation on female social
177 behavior. To test this idea, we employed the TRAP2 activity-dependent labeling strategy to
178 chemogenetically silence POA_{iso} neurons in single-housed females during social interactions
179 with novel, group-housed female visitors (Fig. 2A). Briefly, the POA of TRAP2 female mice
180 was injected bilaterally with a virus driving the Cre-dependent expression of the inhibitory
181 DREADDs receptor hM4Di. Three weeks later, females were single-housed for 3 days and
182 then given a 30-minute social encounter with a novel, group-housed female visitor in their
183 home cage. Following the social interaction, resident females were given an I.P. injection of
184 4-hydroxytamoxifen (4-OHT), which drives the transient expression of Cre recombinase in
185 recently active neurons and thereby enables the expression of hM4Di in POA_{iso} neurons.
186 Subject females remained single-housed for an additional 24 hours and then were re-group-
187 housed with siblings for 2 weeks. Subject females were then single-housed a second time
188 for 3 days and subsequently given a 30-minute same-sex interaction following I.P. injection
189 of either saline (control) or clozapine-n-oxide (CNO) (saline and CNO tests were run 3 days
190 apart, and the order was counterbalanced across experiments).

191 Comparison of the social behaviors of single-housed females between CNO and
192 saline sessions revealed that chemogenetic silencing of POA_{iso} neurons significantly
193 reduced resident-initiated investigation (Fig. 2B; N = 12; red points; two-way ANOVA with
194 repeated measures on one factor; $p < 0.01$). Inhibition of POA_{iso} neurons also tended to
195 reduce mounting, although this effect was not statistically significant (Fig. 2D; Kruskal Wallis
196 test performed on difference in mounting time (CNO-saline) for each group; $p > 0.05$).
197 Finally, inhibition of POA_{iso} neurons significantly reduced USV production (Fig. 2D; two-way
198 ANOVA with repeated measures on one factor; $p < 0.01$). In contrast, CNO treatment did not
199 affect the production of any of these social behaviors in single-housed females with GFP
200 expressed in POA_{iso} neurons (Fig. 2B-D; N = 14; black points; $p > 0.05$ for all CNO vs. saline
201 comparisons in the POA_{iso} FLEX-GFP control group). To investigate the specificity of these
202 effects to chemogenetic silencing of POA_{iso} neurons, we also performed control experiments
203 in which activity-dependent chemogenetic silencing was performed caudal to the POA within
204 the anterior hypothalamus (AH) (Figs. 2B-D; N = 12; brown points) or within the VMH (Fig.
205 2B-D; N = 5; gray points). No significant effects of CNO treatment on resident-initiated
206 investigation, mounting, or USV rate were observed in these control groups (Figs. 2C-D; $p >$
207 0.05 for all). The effect of chemogenetic inhibition of POA_{iso} neurons to decrease female
208 social behavior also cannot be attributed to an overall decrease in movement (Fig. 2E; $p >$
209 0.5 for difference in movement between saline and CNO sessions; see Methods). In
210 summary, we demonstrate that chemogenetic silencing of POA_{iso} neurons attenuates
211 isolation-induced changes in social behavior in female mice.

212 **Ablation of POA_{iso} neurons attenuates the effects of social isolation on female**
213 **mounting**

214 In previous work investigating the role of the POA in regulating rodent social
215 behaviors, studies have reported different effects on behaviors according to whether they
216 employed reversible or irreversible neuronal silencing strategies. Studies that used
217 chemogenetic or optogenetic methods to reversibly silence genetically-defined subsets of
218 POA neurons report decreases in both USV production in males (Chen et al., 2021; Karigo
219 et al., 2021) and in mounting in males and females during interactions with female social
220 partners (Gao et al., 2019; Karigo et al., 2021). In contrast, studies employing caspase-
221 mediated ablation of genetically-defined subsets of POA neurons (Gao et al., 2019; Wei et
222 al., 2018) or electrolytic lesions of the POA (Bean et al., 1981) report decreased mounting
223 but no effects on rates of USV production. To test whether permanent ablation of POA_{iso}
224 neurons attenuates the effects of social isolation on female behavior in a manner similar to
225 the effects of chemogenetic inhibition, we used the TRAP2 activity-dependent labeling
226 strategy to express caspase in and to thereby ablate POA_{iso} neurons (Fig. 3A; see Methods).
227 Vocal and non-vocal social behaviors of resident females were compared pre- and post-
228 ablation, and the same measurements were made in control females expressing GFP in
229 POA_{iso} neurons.

230 In contrast to the effects of chemogenetic inhibition of POA_{iso} neurons, we found that
231 caspase-mediated ablation of POA_{iso} neurons did not affect rates of social investigation in
232 single-housed females, although both experimental and control females spent more time
233 investigating visitors in the post-4-OHT session (Fig. 3B; two-way ANOVA with repeated
234 measures on one factor; $p > 0.05$ for main effect of group, $p < 0.01$ for main effect of time, p
235 > 0.05 for interaction effect). Ablation of POA_{iso} neurons also failed to reduce USV
236 production in pairs containing single-housed females (Fig. 3D; two-way ANOVA with
237 repeated measures on one factor; $p > 0.05$ for pre-4-OHT vs. post-4-OHT USV rates in
238 POA_{iso}-caspase females). Notably, ablation of POA_{iso} neurons significantly reduced
239 mounting in single-housed females (Fig. 3C; Mann Whitney U test performed on the
240 difference in mounting time (post-4-OHT - pre-4-OHT, $p = 0.01$). Taken together with our
241 chemogenetic inhibition data, these results show that both reversible inhibition or irreversible
242 ablation of POA_{iso} neurons in single-housed female mice attenuates the effects of short-term
243 isolation on mounting behavior, whereas only chemogenetic inhibition of POA_{iso} neurons
244 attenuates the effects of short-term isolation on female social investigation and USV
245 production.

246 **Optogenetic activation of POA_{iso} neurons elicits USV production**

247 To understand whether artificial activation of POA_{iso} neurons can recapitulate the
248 effects of short-term isolation on female social behavior, we assessed the effects of
249 optogenetic activation of POA_{iso} neurons on the social behaviors of group-housed females.
250 The TRAP2 strategy was used to express either channelrhodopsin (ChR2) or GFP in POA_{iso}
251 neurons (Fig. 4A; see Methods), and females were re-group-housed for two weeks before
252 beginning optogenetic activation experiments. The effects of optogenetically activating
253 POA_{iso} neurons were first assessed for each subject female in a 5-minute solo session, in
254 which the female was tested alone in a behavior chamber while pulses of blue light were
255 delivered unilaterally to the POA (473 nm, 10 mW, 20-50 Hz, 10-20 ms pulses, 5-10s train
256 durations). The effects of optogenetically activating POA_{iso} neurons were then assessed for
257 each subject female in a 20-minute social session, in which a novel, group-housed female
258 visitor was added to the behavior chamber. The pair was allowed to interact in the absence
259 of optogenetic stimulation for the first and last 5 minutes of the social session, and pulses of
260 blue light were delivered to the POA of the subject female throughout the middle 10 minutes
261 of the session (Fig. 4A).

262 When POA_{iso}-ChR2 females were tested alone, we found that optogenetic activation
263 of POA_{iso} neurons elicited weak-to-moderate USV production in 4 of 8 females, but the
264 comparison of USV rates from pre-laser baseline to the laser stimulation period was not
265 significant at the level of the entire group (Fig. 4B; Mann Whitney U test performed on the
266 difference in USV rates (laser - pre-laser), $p = 0.09$). In POA_{iso}-GFP control females, laser
267 stimulation failed to elicit USV production (0 ± 0 USVs elicited in $N = 6$ POA_{iso}-GFP controls).
268 Interestingly, we found that when laser stimulation was applied during social sessions,
269 optogenetic activation of POA_{iso} neurons more readily elicited USV production than in solo
270 sessions (Fig. 4C; USVs elicited by blue laser stimulation in 7 of 8 POA_{iso}-ChR2 females;
271 Mann Whitney U test performed on the difference in USV rates (laser - pre-laser), $p =$
272 0.006). Moreover, optogenetic activation elicited higher rates of USVs when applied at times
273 when subject females were in close proximity to visitor females (within 2 mouse body
274 lengths) as compared to times when the females were farther apart (mean increase in USV
275 rates from pre-laser to laser period was 2.96 ± 2.32 USVs/s for “near” stimulations, $1.84 \pm$
276 1.75 USVs/s for “far” stimulations; paired t-test performed on the difference in USV rates
277 (laser - pre-laser) for “far” vs. “near” stimulations; $p = 0.02$). In summary, optogenetic
278 activation of POA_{iso} neurons elicits USV production in group-housed females, and the
279 efficacy of this effect is modulated by social context and proximity to a social partner.

280 In contrast to the effects on USV production, optogenetic activation of POA_{iso}
281 neurons failed to extend the duration of social investigation bouts (paired t-test performed on
282 mean duration of social investigation bouts for each POA_{iso}-ChR2 female that overlapped

283 with laser stimulation vs. those that did not; $p > 0.05$). Moreover, optogenetic activation of
284 POA_{iso} neurons only infrequently elicited mounting (activation elicited $n = 1$ bout of mounting
285 in $N = 1$ POA_{iso}-ChR2 female, $n = 2$ bouts of mounting in $N = 1$ POA_{iso}-ChR2 female, and $n =$
286 0 bouts of mounting in the remaining $N = 7$ POA_{iso}-ChR2 females). In summary, optogenetic
287 activation of POA_{iso} neurons elicits USV production from group-housed females, particularly
288 when female subjects are engaged in interactions with female visitors, but otherwise fails to
289 recapitulate the effects of short-term isolation on the social behaviors of female mice.

290 Previous studies have found that USV production can be elicited in female and male
291 mice by artificial activation of VGAT⁺ POA neurons (Gao et al., 2019), Esr1⁺ POA neurons
292 (which are predominantly VGAT⁺) (Chen et al., 2021; Michael et al., 2020), as well as POA
293 neurons that send axonal projections to the caudolateral PAG (which are predominantly
294 VGAT⁺) (Chen et al., 2021; Michael et al., 2020). To ask to what extent POA_{iso} neurons
295 overlap with these previously described populations, we first evaluated the neurotransmitter
296 phenotype of POA_{iso} neurons by performing two-color in situ hybridization for c-fos mRNA
297 and vesicular GABA transporter (VGAT) mRNA and calculating the percentage of Fos⁺ POA
298 neurons that co-expressed VGAT. This analysis revealed that a majority of POA_{iso} neurons
299 are GABAergic (Fig. S2A-B; $N = 4$, $76 \pm 8.8\%$). We next used the TRAP2 activity-dependent
300 labeling strategy to express GFP in POA_{iso} neurons and found GFP-positive axons within the
301 caudolateral PAG, indicating that at least some POA_{iso} neurons send axonal projections to
302 the PAG (Fig. S2C-D; see Methods). Finally, we combined retrograde tracing from the
303 caudolateral PAG with Fos immunostaining to quantify the percentage of PAG-projecting
304 POA neurons that increase Fos expression in single-housed females following same-sex
305 interactions. This experiment revealed that around 20% of PAG-projecting POA neurons
306 express Fos in single-housed females following same-sex interactions (Fig. S2E-F; $N = 4$
307 females, percentage of tdTomato neurons that are Fos-positive = $18.3 \pm 2.9\%$). These
308 findings suggest that a subset of POA_{iso} neurons overlap with GABAergic, PAG-projecting
309 POA neurons that have been demonstrated in previous work to promote USVs via
310 disinhibition of excitatory PAG neurons important to USV production (Chen et al., 2021;
311 Michael et al., 2020).

312 **POA neurons increase their activity in single-housed male mice following opposite-** 313 **sex but not same-sex social interactions**

314 Given our findings that POA_{iso} neurons contribute to isolation-induced changes in the
315 social behaviors of female mice, we next wondered whether a similar population of POA
316 neurons contributes to isolation-induced changes in social behavior in male mice. To
317 address these questions, we measured the vocal and non-vocal social behaviors of sexually
318 naïve males, which were either group-housed with same-sex siblings or single-housed for

319 three days and then given a 30-minute social interaction with a novel, group-housed visitor.
320 To consider the effects of isolation on male social behavior in different social contexts, males
321 were given either a social encounter with a same-sex visitor (MM context) or with an
322 opposite-sex visitor (MF context). Following these social interaction tests, we collected the
323 brains of the subject males and performed immunostaining to measure Fos expression
324 within the POA. Consistent with our prior work (Zhao et al., 2021), we found that males
325 exhibit higher rates of social investigation, higher rates of mounting, and produce more
326 USVs during interactions with females than during same-sex interactions (Fig. 5A-C; $p <$
327 0.05 for main effect of social context for all three behaviors). With respect to resident-
328 initiated investigation, we found a significant main effect of housing, indicating that single-
329 housed males spent more time investigating visitors during both opposite-sex and same-sex
330 interactions (Fig. 5A; two-way ANOVA, $p = 0.02$ for main effect of housing). In contrast,
331 single-housed males spent more time mounting female visitors than did group-housed
332 males, but there were no differences in mounting between single-housed and group-housed
333 males during same-sex interactions (Fig. 5B; two-way ANOVA, $p < 0.05$ for difference
334 between single-housed males interacting with females and all other groups). Similarly, there
335 was also a context-dependent effect of social isolation on male USV production, whereby
336 only single-housed males that interacted with female visitors exhibited increased USV
337 production relative to group-housed males (Fig. 5C; two-way ANOVA with post-hoc Tukey's
338 HSD tests; $p < 0.001$ for total USVs in single-housed MF vs. group-housed MF trials; $p >$
339 0.05 for total USVs in single-housed MM vs. group-housed MM trials). The finding that short-
340 term isolation exerts larger effects on male social behavior during subsequent opposite-sex
341 interactions relative to same-sex interactions is consistent with prior work (Zhao et al., 2021).
342 When we examined POA Fos expression in these four groups of males, we found that POA
343 Fos was significantly elevated in single-housed males following interactions with females
344 relative to the other three groups (Fig. 5D; two-way ANOVA, Tukey's post-hoc HSD tests; p
345 < 0.05 for difference in POA Fos between single-housed MF and all other groups). In
346 summary, the effects of short-term isolation on male social behavior are context-dependent,
347 and increased Fos expression within the POA is seen in single-housed males following
348 interactions with females, a context marked by increased male social investigation,
349 increased male mounting, and increased male USV production.

350 To test whether neural activity in male POA_{iso} neurons contributes to isolation-
351 induced changes in male social behavior, we used the TRAP2 strategy to chemogenetically
352 silence POA_{iso} neurons in single-housed males during social interactions with novel, group-
353 housed females (see Methods). The vocal and non-vocal behaviors of subject males were
354 measured and compared during 30-minute social interactions following I.P. injection of either

355 saline or CNO. Control males were treated identically but were injected with a virus to drive
356 expression of GFP in POA_{iso} neurons. In contrast to our findings in females, chemogenetic
357 inhibition of male POA_{iso} neurons tended to reduce time spent mounting (Fig. 5G; Mann
358 Whitney U test performed on difference in mounting time (CNO - saline); $p = 0.13$ for
359 difference between groups) but did not change rates of resident-initiated social investigation
360 (Fig. 5F; two-way ANOVA with repeated measures on one factor; $p = 0.01$ for main effect of
361 group; $p > 0.05$ for main effect of drug and for interaction effect) and also did not affect USV
362 rates (Fig. 5H; two-way ANOVA with repeated measures on one factor; $p > 0.05$ for main
363 effects and interaction effect). In summary, we find that chemogenetic silencing of male
364 POA_{iso} neurons tends to reduce mounting during subsequent social interactions with females
365 but does not reduce social investigation or USV production, a pattern of results that differs
366 from the effects on single-housed female social behavior of chemogenetically silencing
367 female POA_{iso} neurons.

368 **Discussion**

369 In the current study, we identify and characterize a population of preoptic
370 hypothalamic neurons that contribute to the effects of short-term social isolation on the
371 social behaviors of mice. These POA_{iso} neurons exhibit increased Fos expression in single-
372 housed female mice following same-sex social interactions, and this increase in Fos
373 expression scales positively with the time females spend investigating and mounting female
374 visitors and tends also to scale with rates of USVs. Chemogenetic silencing of POA_{iso}
375 neurons attenuates the effects of social isolation on female social behavior, significantly
376 reducing social investigation and USV production while tending to reduce mounting. In
377 contrast, irreversible ablation of POA_{iso} neurons significantly reduces mounting in single-
378 housed females but has no effect on rates of social investigation or USVs. Optogenetic
379 activation of POA_{iso} neurons partially recapitulates the effects of short-term isolation on
380 female behavior and promotes USV production in female mice, particularly during same-sex
381 social interactions and when in close proximity to female visitors. Finally, we extended our
382 analyses to male mice to understand whether similar POA neurons may mediate changes in
383 male social behavior following short-term isolation. We find that short-term isolation exerts
384 more robust effects on male behavior during subsequent interactions with females than
385 during subsequent interactions with males, and increased POA Fos expression is only seen
386 in single-housed males following social interactions with females. Interestingly,
387 chemogenetic silencing of these POA_{iso} neurons tends to reduce mounting but has no effect
388 on social investigation and USV production, in contrast to the effects of chemogenetically
389 silencing POA_{iso} neurons in females. Together, these experiments identify a population of

390 preoptic hypothalamic neurons that promote social behaviors in single-housed mice in a
391 manner that depends on sex and social context.

392 An extensive body of past work has implicated the POA in the regulation of male
393 sexual behavior, including in the regulation of male courtship vocalizations in both rodents
394 and birds (Alger and Ritters, 2006; Bean et al., 1981; Gao et al., 2019; Merari and Ginton,
395 1975; Ritters, 2012; Ritters et al., 2000; Ritters and Ball, 1999; Wei et al., 2018). Past work
396 has also shown that activation of genetically-defined subsets of POA can elicit the
397 production of USVs in both male and female mice (Chen et al., 2021; Gao et al., 2019;
398 Karigo et al., 2021; Michael et al., 2020). However, whether the POA regulates natural USV
399 production in female mice remained unclear. In the current study, we demonstrate that
400 reversible silencing of POA neurons that increase their activity during same-sex interactions
401 decreases female USV production, indicating that the POA regulates the production of USVs
402 by single-housed females engaged in same-sex interactions. Whether these same neurons
403 regulate female USV production in other behavioral contexts, including in group-housed
404 females and in females interacting with male partners, remains an important open question.
405 In addition to attenuating USV production, we found that silencing of POA_{iso} neurons in
406 single-housed females significantly reduced social investigation of a same-sex partner and
407 also tended to reduce mounting. Our retrograde and anterograde tracing experiments
408 demonstrate that at least a subset of POA_{iso} neurons project to the caudolateral PAG where
409 neurons important for USV production reside, and an attractive possibility is that POA_{iso}
410 neurons promote USV production via disinhibition of PAG-USV neurons as previously
411 demonstrated for genetically-defined subsets of POA neurons (Chen et al., 2021; Michael et
412 al., 2020; Tschida et al., 2019). Future experiments will be required to determine whether
413 PAG-projecting POA_{iso} neurons also regulate social investigation and mounting, or
414 alternatively, whether distinct molecularly-defined or projection-defined subsets of POA_{iso}
415 neurons differentially regulate these different aspects of female social behavior. The latter
416 organization would be reminiscent of how projection-defined subsets of galanin-expressing
417 POA neurons regulate different aspects of parental behavior (Kohl et al., 2018).

418 Although reversible inhibition of POA_{iso} neurons reduced both social investigation and
419 USV production in single-housed females, permanent caspase-mediated ablation of these
420 neurons significantly reduced mounting but had no effects on social investigation or USV
421 production. These differences are largely consistent with prior studies that reported effects
422 on both mounting and USV production following reversible manipulations of POA activity and
423 effects on mounting but not on USV production following irreversible manipulations of POA
424 activity (Bean et al., 1981; Chen et al., 2021; Gao et al., 2019; Karigo et al., 2021; Wei et al.,

2018). One possibility is that POA_{iso} neurons do not directly regulate USV production but rather that reversible silencing of these neurons causes off-target disruptions of neural activity in interconnected brain regions that in turn directly regulate USV production. Such a relationship was demonstrated for motor cortex, whereby reversible silencing of motor cortex disrupted performance of a learned forelimb reaching task in rats, while permanent lesions of motor cortex had no effect on task performance after learning (Otchy et al., 2015). However, our finding that optogenetic activation of POA_{iso} neurons elicits USV production, along with past work demonstrating that POA activation elicits USV production (Chen et al., 2021; Gao et al., 2019; Karigo et al., 2021; Michael et al., 2020) supports the idea that the POA directly regulates USV production. An alternative explanation for the apparently contradictory effects of chemogenetic silencing vs. ablation of POA_{iso} neurons is that while the POA plays an obligatory role in mounting behavior (at least in certain contexts, see below), compensatory changes in additional, non-POA circuits that promote USV production (and social investigation) are sufficient to compensate for the permanent loss of POA_{iso} neurons, leaving these behaviors unperturbed following POA_{iso} neuronal ablation. The identification of forebrain-to-midbrain circuits that regulate USV production in both females and males remains an important future goal.

Our finding that POA_{iso} neurons regulate female-female mounting extends recent work examining the role of hypothalamic regions in regulating male mounting behavior in different social contexts (Karigo et al., 2021). Although the POA plays a well-established role in the regulation of mounting behavior by male rodents during interactions with females, interactions which are typically marked by high rates of USV production and are considered affiliative, the authors found that the VMH regulates male mounting behavior during interactions with other males, which is typically not accompanied by USV production and often precedes fighting. Taken together with the findings of the current study, we conclude that the POA regulates mounting behavior in both male and female mice that is directed toward female social partners and is accompanied by USV production. The question of whether the social behaviors exhibited by single-housed female mice during same-sex interactions are indeed affiliative and how these behaviors shape future interactions with female social partners are important questions that remain to be addressed. Although chemogenetic silencing of POA_{iso} neurons tended to reduce female mounting and ablation of POA_{iso} neurons significantly reduced female mounting, we were not able to reliably elicit mounting behavior through optogenetic activation of POA_{iso} neurons (optogenetically-elicited mounting was observed in n = 3 laser stimulations across N = 2 POA_{iso}-ChR2 females). We note that previous studies that elicited mounting in male mice via optogenetic activation of either Esr1⁺ POA neurons or POA neurons that co-express Esr1 and VGAT used longer

461 laser stimulation trains (15-30s) than we employed in the current study (Karigo et al., 2021;
462 Wei et al., 2018). It is possible that longer periods of optogenetic activation of POA_{iso}
463 neurons would be more effective in eliciting mounting in group-housed females, and another
464 possibility is that POA_{iso} neurons overlap somewhat but not perfectly with the genetically-
465 defined groups of POA neurons manipulated in those prior studies. Regardless, our finding
466 that optogenetic activation of POA_{iso} neurons promotes USV production efficaciously relative
467 to mounting indicates that effects on USV production are not secondary to effects on other
468 female social behaviors.

469 To understand whether a similar population of POA neurons might regulate changes
470 in social behavior following short-term isolation in males, we extended our experiments to
471 single-housed males that subsequently interacted with either a male social partner or with a
472 female social partner. Consistent with our prior work (Zhao et al., 2021), we found that short-
473 term isolation exerts more robust on the effects of male behavior during subsequent
474 interactions with females than during interactions with males. Although single-housed males
475 exhibited increased rates of social investigation while interacting with both males and
476 females relative to group-housed males, single-housed males that interacted with females
477 exhibited increases in all measured social behaviors (social investigation, USV production,
478 and mounting), a pattern of behavioral changes that is similar to what we observed in single-
479 housed females. We also observed that a population of POA neurons increased Fos
480 expression in single-housed males following interactions with female visitors but not
481 following interactions with male visitors. Unexpectedly, we found that the effects of
482 chemogenetically inhibiting POA_{iso} neurons in males differed from those in females. Namely,
483 while reversible inhibition of POA_{iso} neurons tended to reduce mounting during interactions
484 between single-housed subject males and female visitors, there were no effects on rates of
485 social investigation and USV production. These findings differ also from recent work showing
486 that chemogenetic inhibition (Chen et al., 2021) or optogenetic inhibition (Karigo et al., 2021)
487 of Esr1⁺ POA neurons reduces USV production in male mice. Although the factors that
488 account for this difference in results are unclear, one possibility is that our TRAP2-based
489 viral labeling in males is biased toward POA neurons that regulate mounting as compared to
490 POA neurons that regulate USV production, although as stated above, more work is
491 required to understand whether these different social behaviors are regulated by distinct or
492 overlapping subsets of POA neurons. Future experiments can also explore to what extent
493 female and male POA_{iso} neurons represent molecularly, anatomically, and functionally
494 similar or dissimilar neuronal populations.

495 The current study adds to an emerging body of literature implicating the POA in the
496 regulation of social behavior in both females and males, including in non-sexual social
497 contexts (Fukumitsu et al., 2022; Hu et al., 2021; Liu et al., 2023; McHenry et al., 2017; Wu
498 et al., 2021). Our findings also complement recent work that has described a role for the
499 POA in regulating behavioral responses to social isolation in female mice. A recent study
500 using BALB/c mice found that reunion with same-sex cagemates following short-term
501 “somatic isolation” (i.e., separation from cagemates via a partition that permits visual,
502 auditory, and olfactory signaling but prevents physical contact) increases the activity of
503 calcitonin-receptor (Calcr) expressing POA neurons (Fukumitsu et al., 2023). Knockdown of
504 Calcr expression in these neurons reduced social-seeking behaviors directed at the cage
505 partition exhibited by single-housed females, and chemogenetic activation of these neurons
506 increased partition-biting behavior in single-housed females. Another recent study using
507 female FVB/NJ mice applied a TRAP2-based intersectional approach to identify POA
508 neurons that increase their activity following reunion with same-sex cagemates (MPN_{reunion}
509 neurons) (Liu et al., 2023). Optogenetic activation of these neurons did not alter social
510 investigation in group-housed females, whereas activation of these neurons during reunion
511 with cagemates following short-term social isolation decreased social investigation.
512 However, optogenetic inhibition of MPN_{reunion} during reunion did not alter rates of social
513 investigation in single-housed females. Although we did not test the effects of activating
514 POA_{iso} neurons in single-housed females in the current study, the difference in the effects of
515 inhibiting POA_{iso} neurons on the behavior of single-housed females (reduced rates of social
516 investigation, USV production, and mounting) relative to the effects of optogenetic inhibition
517 of MPN_{reunion} neurons in Liu et al. (no effect on social investigation during reunion) suggest
518 that these may represent distinct populations of POA neurons. We note that in the current
519 study, single-housed female subjects remained single-housed for 24 hours following social
520 interaction TRAPing sessions, a design intended to maximize viral labeling of POA neurons
521 that promote increased female social behaviors and that would likely in turn minimize viral
522 labeling of POA neurons that promote social satiety. Taken together, these studies highlight
523 a complex role for the POA in regulating multiple aspects of changes in social behavior
524 following short-term social isolation. Although some studies of social isolation have avoided
525 the use of C57BL/6J female mice, the robust triad of changes in social behavior exhibited by
526 these females following short-term isolation affords a powerful opportunity to continue
527 investigating neural circuit mechanisms through which short-term social isolation promotes
528 social behaviors, as well as to investigate how hypothalamic circuits regulate the
529 coordinated production of suites of social behaviors during female-female social interactions.

530

531 **Acknowledgements:** Thanks to Frank Drank and other CARE staff for their excellent
532 mouse husbandry. All experimental design schematics included in the figures were created
533 with Biorender.com.

534

535 **Author contributions:** X.Z. and K.A.T. designed the experiments. X.Z. and Y.C. conducted
536 the experiments. X.Z., Y.C., D.S., V.C., D.D., J.W.S., A.S., and K.A.T. analyzed data. X.Z.
537 and K.A.T. wrote the manuscript, and all authors approved the final version.

538

539 **Declaration of Interests:** The authors declare no competing interests.

540 **Figure legends**

541 **Figure 1. The POA contains neurons that increase Fos expression in single-housed**
542 **females following same-sex interactions.** (A) Schematic of experiment to measure Fos
543 expression in group-housed and single-housed females following same-sex social
544 interactions. (B) Total time spent engaged in resident-initiated social investigation for group-
545 housed residents (teal) and single-housed residents (maroon). (C) Same as (B), for total
546 resident-initiated mounting time. (D) Same as (B), for total USVs recorded from pairs
547 containing group-housed or single-housed residents. (E) Left-most image shows the location
548 of the POA in a coronal brain section. Representative confocal images show Fos expression
549 (green) in the POA of a group-housed female (left) and a single-housed female (right)
550 following same-sex social interactions. Blue, Neurotrace. (F) Quantification of Fos-positive
551 neurons is shown for the POA (left), the VMH (middle), and the caudolateral PAG (right) for
552 group-housed and single-housed females. Open bars show data from females that did not
553 engage in social interactions with novel females (baseline), and closed bars show data from
554 females following social interactions with novel females (interaction). (G) Total time spent in
555 resident-initiated interaction is plotted for 14-day single-housed (maroon) and re-group-
556 housed females (teal) during same-sex interactions that occurred prior to isolation (day 0),
557 following 3 days of isolation (day 3), and on the test day (day 17). (H) Same as (G), for total
558 resident-initiated mounting time. (I) Same as (G), for total USVs. (J) Quantification of Fos-
559 positive POA neurons is shown for 14-day single-housed females (maroon) and re-group-
560 housed females (teal).

561 **Figure 2. Effects of chemogenetic inhibition of POA_{iso} neurons on the social behaviors**
562 **of single-housed female mice.** (A) Experimental timeline and viral strategy to
563 chemogenetically inhibit the activity of POA_{iso} neurons in single-housed females. (B) Total
564 time spent in resident-initiated social investigation is shown on saline and CNO days for 4
565 experimental groups: (red symbols) experimental females in which hM4Di is expressed in
566 POA_{iso} neurons; (black symbols) control females in which GFP is expressed in POA_{iso}
567 neurons; (brown symbols) control females in which hM4Di is expressed in 'TRAPed' AH
568 neurons; (gray symbols) control females in which hM4Di is expressed in 'TRAPed' VMH
569 neurons. (C) Same as (B), for total duration of resident-initiated mounting. (D) Same as (B),
570 for total USVs. (E) Total movement is plotted for females with hM4Di expressed in POA_{iso}
571 neurons, on saline days vs. CNO days.

572 **Figure 3. Effects of caspase-mediated ablation of POA_{iso} neurons on the social**
573 **behaviors of single-housed female mice.** (A) Experimental timeline and viral strategy for
574 caspase-mediated ablation of POA_{iso} neurons in single-housed females. (B) Total time spent

575 in resident-initiated social investigation is shown pre- and post-4-OHT treatment for 2
576 experimental groups: (red symbols) experimental females in which caspase is expressed in
577 POA_{iso} neurons; (black symbols) control females in which GFP is expressed in POA_{iso}
578 neurons. (C) Same as (B), for total duration of resident-initiated mounting. (D) Same as (B),
579 for total USVs.

580 **Figure 4. Effects of optogenetic activation of POA_{iso} neurons on the behaviors of**
581 **group-housed female mice.** (A) Experimental timeline and viral strategy to optogenetically
582 activate POA_{iso} neurons in group-housed females. (B) Mean total USVs produced during
583 social sessions shown for pre-laser periods and during laser stimulation periods for
584 experimental females with ChR2 expressed in POA_{iso} neurons (red symbols; N = 9) and for
585 control females with GFP expressed in POA_{iso} neurons (black symbols, N = 6). (C) Same as
586 (B), for social sessions. (D) Spectrograms are shown from a representative POA_{iso}-ChR2
587 female to illustrate USVs that were elicited through optogenetic activation of POA_{iso} neurons
588 in a solo session (top) and a social session (bottom). Blue bars indicate timing of laser
589 stimulation.

590 **Figure 5. Context-dependent differences in POA Fos expression and effects of**
591 **chemogenetic inhibition of POA_{iso} neurons on the social behaviors of single-housed**
592 **male mice.** (A) Total time spent in resident-initiated social investigation is shown for group-
593 housed male residents (teal) and single-housed male residents (maroon) during interactions
594 with either female visitors (left) or male visitors (right). (B) Same as (A), for total resident-
595 initiated mounting time. (C) Same as (A), for total USVs recorded from pairs containing
596 group-housed or single-housed male residents. (D) Total number of Fos-positive POA
597 neurons is shown for group-housed male residents (teal) and single-housed male residents
598 (maroon) following interactions with female visitors (left) or male visitors (right). (E)
599 Experimental timeline and viral strategy to chemogenetically inhibit the activity of POA_{iso}
600 neurons in single-housed males. (F) Total time spent in resident-initiated social investigation
601 is shown on saline and CNO days for experimental males in which hM4Di is expressed in
602 POA_{iso} neurons (red symbols, N = 7) and control males in which GFP is expressed in POA_{iso}
603 neurons (black symbols, N = 7). (G) Same as (F), for total duration of resident-initiated
604 mounting. (H) Same as (F), for total USVs.

605 **Materials and methods**

606 **Key Resources**

REAGENT or RESOURCE	SOURCE	IDENTIFIER
Antibodies		
c-Fos (9F6) Rabbit mAb	Cell Signaling Technology	2250S
Alexa Fluor 488 goat-anti-rabbit	Invitrogen	A-11008
Neurotrace 435/455 Blue	Thermo Fischer Scientific	CAT#: N21479
Commercial assay or kit		
HCR v3.0	Molecular Instruments	
Bacterial and Virus Strains		
AAV2/1-hSyn-FLEX-hM4Di-mCherry	Addgene	RRID: Addgene_44262
AAV2/1-Ef1alpha-hChR2(h134R)-EYFP-WPRE-HGHpA	Addgene	RRID: Addgene_20298
AAVrg-pgk-Cre	Addgene	RRID: Addgene_24593
pAAV-flex-taCasp3-TEVp	Addgene	RRID: Addgene_45580
AAV2/1-pCAG-FLEX-EGFP-WPRE	Addgene	RRID: Addgene_51502
Chemicals, Peptides, and Recombinant Proteins		
Clozapine N-oxide dihydrochloride	Hello Bio	HB6149; E1458-2-1
4-Hydroxytamoxifen	Hello Bio	HB6040
Experimental Models: Organisms/Strains		
<i>TRAP2 Fos^{tm2.1(cre/ER12)Lox/J}</i>	Jackson Labs	IMSR_JAX:030323
<i>Ai14 B6.CgGt(ROSA)26Sor^{tm14(CAG-tdTomato)Hze/J}</i>	Jackson Labs	IMSR_JAX:007914
C57BL/6J	Jackson Labs	IMSR_JAX:000664
Software and Algorithms		
MATLAB	Mathworks	http://www.mathworks.com RRID: SCR_001622
ZEN	Zeiss	https://www.zeiss.com RRID:SCR_013672
Spike2	CED	http://ced.co.uk RRID:SCR_000903
ImageJ	NIH	https://imagej.net/ij/ RRID:SCR_003070
Behavioral Observation Research Interactive Software	Open Behavior	https://github.com/olivierfriard/BORIS RRID:SCR_021509
R Project for Statistical Computing	R Core Team	http://www.r-project.org/ RRID:SCR_001905
R Studio	Posit	https://posit.co/ RRID:SCR_000432

607

608 **Lead contact**

609 Further information and requests for resources should be directed to and will be fulfilled by
610 the lead contact, Katherine Tschida (kat227@cornell.edu).

611 **Experimental models and subject details**

612 **Animal statement**

613 All experiments and procedures were conducted according to protocols approved by the
614 Cornell University Institutional Animal Care and Use Committee (protocol #2020-001).

615 **Animals**

616 TRAP2 (Jackson Laboratories, 030323) and Ai14 (Jackson Laboratories, 007914) mice were
617 at least 8 weeks old at the time of the experiments or surgeries. TRAP2;Ai14 mice were
618 generated by crossing TRAP2 with Ai14. All mice were kept on a 12:12 reversed light/dark
619 cycle, were housed in ventilated micro-isolator cages in a controlled environment with
620 regulated temperature and humidity, and were provided with unrestricted access to food and
621 water. A running wheel (Innovive) was present in all homecages from the time of weaning
622 and was subsequently removed immediately before initiating the social interaction test.
623 Mouse cages were cleaned weekly, and experiments were never conducted on cage change
624 days.

625 **Methods details**

626 **Social isolation and social interaction tests**

627 Female and male subject mice were either group-housed with same-sex siblings or
628 separated from their cage mates and individually housed in clean cages for three days prior
629 to behavioral tests. In the case of group-housed subject mice, siblings were temporarily
630 removed from the home cage for the duration of the test. The subject animal's home cage
631 was then placed in a sound-attenuating recording chamber (Med Associates) equipped with
632 an ultrasonic microphone (Avisoft), an infrared light source (Tendelux), and a webcam
633 (Logitech, with the infrared filter removed to enable video recording under infrared lighting
634 conditions). A novel, group-housed visitor mouse (female or male mouse on a C57BL/6
635 background) was placed in the home cage of the subject mouse, and vocal and non-vocal
636 behaviors were recorded for 30 minutes. Visitor mice were used across multiple experiments
637 (< 6 in total), including in interactions with both group-housed and single-housed subject
638 mice. Visitor females used in male-female interactions were never used for female-female
639 experiments, but a subset of visitors used in female-female interactions were subsequently
640 used in male-female experiments.

641 A separate cohort of female mice was used to investigate the effects on social behavior of
642 re-group-housing following a period of social isolation. For this cohort of mice, social

643 interaction tests with novel, group-housed female visitors were conducted at three
644 timepoints: (1) on day 0, when subject females were still group-housed; (2) On day 3, after
645 being single-housed for 3 days; (3) on day 17, after a randomly selected subset of subject
646 females were re-group-housed with their siblings for two weeks, and the remaining female
647 subjects remained single-housed for two weeks.

648 **USV recording and detection**

649 USVs were recorded with an ultrasonic microphone (Avisoft, CMPA/CM16), amplified
650 (Presonus TubePreV2), and digitized at 250 kHz (Avisoft UltrasoundGate 166H or CED
651 Power 1401). USVs were detected with custom MATLAB codes (Tschida et al., 2019) using
652 the following parameters (mean frequency > 45 kHz; spectral purity > 0.3; spectral
653 discontinuity < 1.00; minimum USV duration = 5 ms; minimum inter-syllable interval = 30
654 ms).

655 **Analyses of non-vocal social behaviors**

656 Trained observers used BORIS software (v.8.13; Friard and Gamba, 2016) to score the
657 following non-vocal behaviors: resident-initiated social investigation and resident-initiated
658 mounting. Social investigation included sniffing and following. Resident-initiated mounting of
659 the visitor typically occurred following a period of resident-initiated social investigation, with
660 the resident mouse positioning its forelimbs on top of the body of the visitor, sometimes with
661 pelvic thrusts and sometimes without. Neither visitor-initiated mounting nor fighting were
662 observed in our dataset.

663 In some trials, total movement was estimated using a custom MATLAB code that allows the
664 user to mark the position of a mouse in every 30th frame (i.e., once per second). Total
665 movement was then calculated as the sum of changes in position across pairs of marked
666 frames.

667 **Fos immunohistochemistry**

668 Two hours following the start of the social interaction test, mice were deeply anesthetized
669 using isoflurane and then transcardially perfused with phosphate-buffered saline (PBS, pH
670 7.4), followed by 4% paraformaldehyde (PFA; Sigma-Aldrich, in 0.1 M PBS, pH 7.4). Brains
671 were subsequently dissected and post-fixed in 4% PFA for 24 hours at 4°C, followed by
672 immersion in 30% sucrose solution in PBS for 48 hours at 4°C. Afterward, brains were
673 embedded in frozen section embedding medium (Surgipath, VWR), flash frozen in a dry ice-
674 ethanol (100%) bath, and then stored at -80°C until sectioning. Sections were cut on a
675 cryostat (Leica CM1950) to a thickness of 80 µm, washed in PBS (3 x 5 mins at RT),

676 permeabilized for 2-3 hours in PBS containing 1% Triton X-100 (PBST), and then blocked in
677 0.3% PBST containing 10% Blocking One (Nacalai USA) for 1 hour at RT on a shaker.
678 Sections were then incubated for 24 hours at 4°C with primary antibody in blocking solution
679 (1:1000 rabbit-anti-Fos, Cell Signaling Technologies, 2250S), washed 3 x 30 minutes in
680 0.3% PBST, then incubated for 24 hours at 4°C with secondary antibody in blocking solution
681 (1:1000, Alexa Fluor 488 goat-anti-rabbit, Invitrogen, plus 1:500 NeuroTrace, Invitrogen)
682 Finally, sections were washed for 2 x 10 minutes in 0.3% PBST, followed by washing for 2 x
683 10 minutes in PBS. After mounting on slides, sections were dried and coverslipped with
684 Fluoromount G (Southern Biotech). Slides were imaged with a 10x objective on a Zeiss 900
685 laser scanning confocal microscope, and Fos-positive neurons within regions of interest
686 were counted manually by trained observers.

687 **Floating section two-color in situ hybridization**

688 In situ hybridization was conducted using hybridization chain reaction (HCR v3.0, Molecular
689 Instruments). Ten minutes after the completion of the 30-minute social interaction tests, mice
690 underwent transcardial perfusion with RNase-free PBS (DEPC-treated), followed by 4%
691 PFA. Dissected brain samples were post-fixed overnight in 4% PFA at 4°C, cryoprotected in
692 a 30% sucrose solution in DEPC-PBS at 4°C for 48 hours, flash frozen in section embedding
693 medium, and stored at -80°C until sectioning. 40 µm-thick coronal floating sections were
694 collected into sterile 24-well plates in DEPC-PBS. These sections were briefly fixed once
695 again for 5 minutes in 4% PFA and subsequently immersed in 70% EtOH in DEPC-PBS
696 overnight. Sections were then rinsed in DEPC-PBS, incubated for 45 minutes in 5% SDS in
697 DEPC-PBS, followed by a series of rinses and incubations: 2x SSCT, pre-incubation in HCR
698 hybridization buffer at 37°C, and incubation in HCR hybridization buffer containing RNA
699 probes (VGAT and Fos) overnight at 37°C. Sections were then rinsed 4 x 15 minutes at
700 37°C in HCR probe wash buffer, rinsed in 2X SSCT, pre-incubated in HCR amplification
701 buffer, and then incubated in HCR amplification buffer containing HCR amplifiers at RT for
702 approximately 48 hours. On the final day, sections were rinsed in 2x SSCT, counterstained
703 with DAPI (Thermo Fisher, 1:5000), rinsed again with 2x SSCT, mounted on slides, and
704 coverslipped with Fluoromount-G (Southern Biotech). After drying, slides were imaged with a
705 10x or 20x objective on a Zeiss 900 laser scanning microscope. Neurons were scored from
706 three sections of tissue from the POA from each mouse, and the absence of presence of
707 staining for different probes was quantified manually by trained scorers.

708 **Viruses**

709 The following viruses and injection volumes were used: AAV2/1-hSyn-FLEX-hM4Di-mCherry
710 (Addgene #44262, 200 nL), AAV2/1-CAG-FLEX-EGFP-WPRE (Addgene #51502, 200 nL),

711 AAV2/5-Ef1alpha-FLEX-taCasp3-TEVp (Addgene #45580, 200 nL), AAV2/1-Ef1alpha-
712 hChr2(h134R)-EYFP-WPRE-HGHpA (Addgene #20298, 200 nL), AAVrg-pgk-Cre (Addgene
713 #24593, 200 nL). The final injection coordinates were as follows: POA, AP = -0.1 mm, ML =
714 0.6 mm, DV = 5.1 mm; AH, AP = -0.7 mm, ML = 0.6 mm, DV = 5.1 mm; VMH, AP = -1.5 mm,
715 ML = 0.7 mm, DV = 5.4 mm; PAG, AP = -4.7 mm, ML = 0.6 mm, DV = 1.75 mm. Viruses
716 were pressure-injected using a pulled glass pipettes mounted in a programmable nanoliter
717 injector (Nanoject III, Drummond) at a rate of 15 nL every 60 s.

718 **Stereotaxic Surgery**

719 Mice were anesthetized using isoflurane (2.5% for induction, then 1.5 - 2.5% for
720 maintenance) and then securely positioned in a stereotaxic apparatus (Angle Two, Leica). A
721 midline incision in the scalp was made to expose the skull, and small craniotomies were
722 created dorsal to each injection site using a surgical drill. Viral injection pipettes were left in
723 place for a minimum of 10 minutes before and after viral injections to minimize backflow
724 upon pipette withdrawal from the brain. Surgical sutures (LOOK 774B, Fisher Scientific) and
725 tissue adhesive (3M) were used to close the incision.

726 For optogenetic activation experiments, an optogenetic ferrule (RWD Fiber Optic Cannula,
727 Ø1.25 mm Ceramic Ferrule, 200 µm Core, 0.22 NA, L = 7 mm) was implanted approximately
728 250 µm above the viral injection site immediately following the viral injection and was
729 secured in place with Metabond (Parkell).

730 **TRAP activity-dependent labeling**

731 Solutions of 4-hydroxytamoxifen (4-OHT, HelloBio, HB6040) were prepared by dissolving 4-
732 OHT powder at 20 mg/mL in ethanol by shaking at 37°C, and aliquots (75 µL) were then
733 stored at -20°C. Before use, 4-OHT was redissolved in ethanol by shaking at 37°C and
734 filtered corn oil was added (150 µL). Ethanol was then evaporated by vacuum under
735 centrifugation to give a final concentration of 10 mg/mL, and the 4-OHT solution was used
736 on the same day it was prepared.

737 To express viral transgenes in recently active neurons, we used the Targeted
738 Recombination in Active Populations (TRAP2) strategy. Two weeks following viral injection,
739 TRAP2 and TRAP2;Ai14 mice were given 30-minute social encounters (as described
740 above). Following the social encounter, subject mice received I.P. injections of 4-OHT (50
741 mg/kg) to enable expression of viral transgenes in recently active neurons. To minimize
742 neural activity triggered by stimuli outside of the social interaction test, all subject animals

743 were individually housed for an additional 24 hours following 4-OHT treatment before being
744 re-group-housed with their same-sex siblings.

745 **Chemogenetic inhibition**

746 To reversibly reduce neuronal activity, TRAP2 female mice received bilateral injections of an
747 Cre-dependent inhibitory DREADDs virus into the hypothalamus (AAV2/1-hSyn-FLEX-
748 hM4Di-mCherry; injected into the POA, AH, or VMH) as described above. TRAP2 male mice
749 received the same viral injections into the POA only. Three weeks later, mice were single-
750 housed for 3 days and then were subsequently given a 30-minute social encounter with a
751 novel, group-housed female visitor. Subject mice then received an I.P. injection of 4-OHT to
752 enable expression of hM4Di in activity-defined populations of hypothalamic neurons. Two
753 weeks later, subject mice received an I.P. injection of either sterile saline (as a control) or
754 clozapine-n-oxide (CNO, 4 mg/kg, Hello Bio HB6149; to inhibit neurons expressing hM4Di)
755 30 minutes prior to a social interaction test. Three days later, mice that previously were
756 treated with saline received an I.P. injection of CNO, and mice that were previously treated
757 with CNO received an I.P. injection of saline, 30 minutes prior to another social interaction.
758 Rates of USV production and non-vocal social behaviors were compared between saline
759 and CNO days within animals to assess the effects of neuronal inhibition on social
760 behaviors. Control mice received unilateral injections into the POA of a Cre-dependent AAV
761 driving the expression of GFP (AAV2/1-CAG-FLEX-EGFP) and were otherwise treated
762 identically to experimental animals.

763 **Neuronal ablation**

764 To permanently ablate neurons, TRAP2;Ai14 female mice received bilateral injections of an
765 AAV2/5-ef1alpha-FLEX-taCasp3-TEVp virus into the POA. Following a three-week recovery
766 period, these animals were individually housed for three days and subsequently given a 30-
767 minute social encounter with a novel, group-housed female visitor. Subject mice then
768 received an I.P. injection of 4-OHT to enable expression of caspase in activity-defined POA
769 neurons. Two weeks later, females were single-housed for three days and then given a
770 second 30-minute social interaction test. Social behaviors of subject females were compared
771 between the pre-ablation and post-ablation interaction tests to assess the effects of neuronal
772 ablation.

773 **Optogenetic activation**

774 Female TRAP2 mice received unilateral injections into the POA of AAV-ef1 α -FLEX-ChR2
775 (experimental) or AAV-CAG-FLEX-GFP (control). In the same surgery, an optogenetic

776 ferrule was implanted approximately 250 μm above the viral injection site. Three weeks later,
777 females were single-housed for 3 days and then given a 30-minute social interaction with a
778 novel group-housed, female visitor. Subject females then received an I.P. injection of 4-
779 OHT. Two weeks later, females were first placed alone in the testing chamber for a 5-minute
780 habituation period after connecting the laser patch cable to the female's optogenetic ferrule.
781 Optogenetic activation sessions consisted of a 5-minute period in which optogenetic
782 activation was performed in solo females, followed by a 20-minute period in which activation
783 was performed as subject females interacted with a novel, group-housed female visitor. The
784 social session was further divided into three phases: 5 minutes without optogenetic
785 activation, 10 minutes with optogenetic activation, and 5 minutes without optogenetic
786 activation. During the middle 10 minutes of the social session, some laser stimuli were
787 delivered at times when the two females were near to one another (inter-animal distance $<$
788 ~ 2 mouse body lengths), and other stimuli were delivered at times when the females were
789 not in close contact. POA_{iso} neurons were optogenetically activated with illumination from a
790 473 nm laser (10 mW) at 20-50 Hz (10-20 ms pulses, trains lasted 5-10s) Laser stimuli were
791 driven by computer-controlled voltage pulses (Spike 2 version 10.8, CED).

792 **Anatomical tracing**

793 Female TRAP2 mice used as GFP controls in the chemogenetic inhibition experiments were
794 subsequently used for anterograde mapping of the axonal projections of POA_{iso} neurons.
795 Three weeks following unilateral injection into the POA of a Cre-dependent AAV driving the
796 expression of GFP (AAV2/1-CAG-FLEX-EGFP), females were single-housed for 3 days and
797 subsequently given a 30-minute social interaction test. Subject mice then received an I.P.
798 injection of 4-OHT. Six weeks later, females were perfused, brains were collected and
799 sectioned, and a confocal microscope was used to image GFP-positive axon terminals
800 within coronal brain tissue sections.

801 To examine the overlap between PAG-projecting POA neurons and Fos expression, Ai14
802 females first received a unilateral injection into the PAG of an AAV driving the retrograde
803 expression of Cre-recombinase (AAVrg-pgk-Cre). Two weeks later, these females were
804 given a 30-minute social interaction test. Ninety minutes after the test, subject females were
805 perfused, brains were collected, and coronal brain sections containing the POA were
806 collected for Fos immunohistochemistry as described above. Brain tissue sections were
807 imaged with a 10x objective on a Zeiss 900 laser scanning confocal microscope, and POA
808 neurons that were Fos-positive and tdTomato-positive were counted manually by trained
809 observers.

810 **Statistics**

811 Two-sided statistical comparisons were used in all analyses ($\alpha = 0.05$). The Shapiro-
812 Wilk test was performed to analyze the normality of each data distribution, and non-
813 parametric statistical tests were used for comparisons that included non-normally distributed
814 data. No statistical methods were used to pre-determine sample size. Mice were only
815 excluded from analysis in cases in which viral injections were not targeted accurately.
816 Details of the statistical analyses used in this study are included in Table S1.

817

818 **Supplemental Information**

819 **Figure S1. Additional characterization of Fos expression in single-housed vs. group-**
820 **housed females and comparison to rates of female social behaviors. (A)**

821 Representative confocal images show Fos expression (green) in the VMH of a group-
822 housed female (left) and a single-housed female (right) following same-sex social
823 interactions. Blue, Neurotrace. (B) Same as (A), for the caudolateral PAG. (C) Left, the
824 relationship between total time spent in resident-initiated social investigation and numbers of
825 Fos-positive POA neurons is shown for group-housed (teal) and single-housed (maroon)
826 female residents following interactions with novel females. Middle, same as left, for total
827 resident-initiated mounting time vs. numbers of Fos-positive POA neurons. Data only shown
828 for single-housed residents because group-housed residents never mounted female visitors.
829 Right, same as left, for total USVs vs. numbers of Fos-positive POA neurons. (D) Left, the
830 relationship between total time spent in resident-initiated social investigation and numbers of
831 Fos-positive VMH neurons is shown for group-housed (teal) and single-housed (maroon)
832 female residents following interactions with novel females. Middle, same as left, for total
833 resident-initiated mounting time vs. numbers of Fos-positive VMH neurons. Right, same as
834 left, for total USVs vs. numbers of Fos-positive VMH neurons. (E) Left, the relationship
835 between total time spent in resident-initiated social investigation and numbers of Fos-
836 positive caudolateral PAG neurons is shown for group-housed (teal) and single-housed
837 (maroon) female residents following interactions with novel females. Middle, same as left, for
838 total resident-initiated mounting time vs. numbers of Fos-positive PAG neurons. Right, same
839 as left, for total USVs vs. numbers of Fos-positive PAG neurons.

840 **Figure S2. Characterization of neurotransmitter phenotype and axonal projections of**

841 **POA_{iso} neurons.** (A) Representative confocal images of in situ hybridization performed on
842 brain sections containing the POA, showing overlap of expression of Fos (green) and VGAT
843 (magenta). Blue, DAPI. (B) Quantification of proportion of Fos-positive POA neurons that
844 expressed VGAT. (C) Experimental timeline and viral strategy to express GFP in POA_{iso}
845 neurons. (D) Confocal images showing GFP-labeled axons of POA_{iso} neurons within the
846 caudolateral PAG. Blue, Neurotrace. (E) Experimental timeline and viral strategy to
847 retrogradely label PAG-projecting POA neurons with tdTomato. (F) Confocal image showing
848 tdTomato labeling in a coronal section containing the POA, and dotted circles in insets
849 indicate examples of double-labeled neurons. Neurotrace, blue. (G) Quantification of
850 proportion of tdTomato-expressing POA neurons that are also Fos-positive.

851 **Table S1. Details of statistical analyses.**

852

853 **References**

- 854 Alger SJ, Riters LV. 2006. Lesions to the medial preoptic nucleus differentially affect singing
855 and nest box-directed behaviors within and outside of the breeding season in European
856 starlings (*Sturnus vulgaris*). *Behav Neurosci* **120**:1326–1336. doi:10.1037/0735-
857 7044.120.6.1326
- 858
859 Allen WE, DeNardo LA, Chen MZ, Liu CD, Loh KM, Fenno LE, Ramakrishnan C, Deisseroth
860 K, Luo L. 2017. Thirst-associated preoptic neurons encode an aversive motivational drive.
861 *Science* **357**:1149–1155. doi:10.1126/science.aan6747
- 862
863 An D, Chen W, Yu D-Q, Wang S-W, Yu W-Z, Xu H, Wang D-M, Zhao D, Sun Y-P, Wu J-C,
864 Tang Y-Y, Yin S-M. 2017. Effects of social isolation, re-socialization and age on cognitive
865 and aggressive behaviors of Kunming mice and BALB/c mice. *Anim Sci J* **88**:798–806.
866 doi:10.1111/asj.12688
- 867
868 Arrigo BA, Bullock JL. 2008. The psychological effects of solitary confinement on prisoners
869 in supermax units: reviewing what we know and recommending what should change. *Int J*
870 *Offender Ther Comp Criminol* **52**:622–640. doi:10.1177/0306624X07309720
- 871
872 Bariselli S, Hörnberg H, Prévost-Solié C, Musardo S, Hatstatt-Burklé L, Scheiffele P, Bellone
873 C. 2018. Role of VTA dopamine neurons and neuregulin 3 in sociability traits related to
874 nonfamiliar conspecific interaction. *Nat Commun* **9**:3173. doi:10.1038/s41467-018-05382-3
- 875
876 Baumeister RF, Leary MR. 1995. The need to belong: Desire for interpersonal attachments
877 as a fundamental human motivation. *Psychol Bull* **117**:497–529. doi:10.1037/0033-
878 2909.117.3.497
- 879
880 Bean NY, Nunez AA, Conner R. 1981. Effects of medial preoptic lesions on male mouse
881 ultrasonic vocalizations and copulatory behavior. *Brain Res Bull* **6**:109–112.
882 doi:10.1016/s0361-9230(81)80033-0
- 883
884 Cacioppo JT, Cacioppo S. 2018. Chapter Three - Loneliness in the Modern Age: An
885 Evolutionary Theory of Loneliness (ETL) In: Olson JM, editor. *Advances in Experimental*
886 *Social Psychology*. Academic Press. pp. 127–197. doi:10.1016/bs.aesp.2018.03.003
- 887
888 Cacioppo JT, Hughes ME, Waite LJ, Hawkley LC, Thisted RA. 2006. Loneliness as a
889 specific risk factor for depressive symptoms: cross-sectional and longitudinal analyses.
890 *Psychol Aging* **21**:140–151. doi:10.1037/0882-7974.21.1.140
- 891
892 Check JVP, Perlman D, Malamuth NM. 1985. Loneuness and Aggressive Behaviour. *J Sol*
893 *Pers Relat* **2**:243–252. doi:10.1177/0265407585023001
- 894
895 Chen J, Markowitz JE, Lilascharoen V, Taylor S, Sheurpukdi P, Keller JA, Jensen JR, Lim
896 BK, Datta SR, Stowers L. 2021. Flexible scaling and persistence of social vocal
897 communication. *Nature* **593**:108–113. doi:10.1038/s41586-021-03403-8
- 898
899 Chevallier C, Kohls G, Troiani V, Brodtkin ES, Schultz RT. 2012. The Social Motivation
900 Theory of Autism. *Trends Cogn Sci* **16**:231–239. doi:10.1016/j.tics.2012.02.007
- 901
902 Clements CC, Zoltowski AR, Yankowitz LD, Yerys BE, Schultz RT, Herrington JD. 2018.
903 Evaluation of the Social Motivation Hypothesis of Autism. *JAMA Psychiatry* **75**:797–808.
904 doi:10.1001/jamapsychiatry.2018.1100
- 905

- 906 Dai B, Sun F, Tong X, Ding Y, Kuang A, Osakada T, Li Y, Lin D. 2022. Responses and
907 functions of dopamine in nucleus accumbens core during social behaviors. *Cell Rep*
908 **40**:111246. doi:10.1016/j.celrep.2022.111246
909
- 910 DeNardo LA, Liu CD, Allen WE, Adams EL, Friedmann D, Fu L, Guenther CJ, Tessier-
911 Lavigne M, Luo L. 2019. Temporal Evolution of Cortical Ensembles Promoting Remote
912 Memory Retrieval. *Nat Neurosci* **22**:460–469. doi:10.1038/s41593-018-0318-7
913
- 914 Dölen G, Darvishzadeh A, Huang KW, Malenka RC. 2013. Social reward requires
915 coordinated activity of nucleus accumbens oxytocin and serotonin. *Nature* **501**:179–184.
916 doi:10.1038/nature12518
917
- 918 Floody OR. 1989. Dissociation of hypothalamic effects on ultrasound production and
919 copulation. *Physiol Behav* **46**:299–307. doi:10.1016/0031-9384(89)90271-0
920
- 921 Fukumitsu K, Huang AJ, McHugh TJ, Kuroda KO. 2023. Role of Calcr expressing neurons in
922 the medial amygdala in social contact among females. *Mol Brain* **16**:10. doi:10.1186/s13041-
923 023-00993-4
924
- 925 Fukumitsu K, Kaneko M, Maruyama T, Yoshihara C, Huang AJ, McHugh TJ, Itohara S,
926 Tanaka M, Kuroda KO. 2022. Amylin-Calcitonin receptor signaling in the medial preoptic
927 area mediates affiliative social behaviors in female mice. *Nat Commun* **13**:709.
928 doi:10.1038/s41467-022-28131-z
929
- 930 Gao S-C, Wei Y-C, Wang S-R, Xu X-H. 2019. Medial Preoptic Area Modulates Courtship
931 Ultrasonic Vocalization in Adult Male Mice. *Neurosci Bull* **35**:697–708. doi:10.1007/s12264-
932 019-00365-w
933
- 934 Green DB, Shackleton TM, Grimsley JMS, Zobay O, Palmer AR, Wallace MN. 2018.
935 Communication calls produced by electrical stimulation of four structures in the guinea pig
936 brain. *PLoS One* **13**:e0194091. doi:10.1371/journal.pone.0194091
937
- 938 Gunaydin LA, Grosenick L, Finkelstein JC, Kauvar IV, Fenno LE, Adhikari A, Lammel S,
939 Mirzabekov JJ, Airan RD, Zalocusky KA, Tye KM, Anikeeva P, Malenka RC, Deisseroth K.
940 2014. Natural neural projection dynamics underlying social behavior. *Cell* **157**:1535–1551.
941 doi:10.1016/j.cell.2014.05.017
942
- 943 Hashikawa K, Hashikawa Y, Tremblay R, Zhang J, Feng JE, Sabol A, Piper WT, Lee H,
944 Rudy B, Lin D. 2017. Esr1+ cells in the ventromedial hypothalamus control female
945 aggression. *Nat Neurosci* **20**:1580-1590. doi:10.1038/nn.4644
946
- 947 Hossain MM, Sultana A, Purohit N. 2020. Mental health outcomes of quarantine and
948 isolation for infection prevention: a systematic umbrella review of the global evidence.
949 *Epidemiol Health* **42**. doi:10.4178/epih.e2020038
950
- 951 House JS, Landis KR, Umberson D. 1988. Social relationships and health. *Science*
952 **241**:540–545. doi:10.1126/science.3399889
953
- 954 Hu RK, Zuo Y, Ly T, Wang J, Meera P, Wu YE, Hong W. 2021. An amygdala-to-
955 hypothalamus circuit for social reward. *Nat Neurosci* **24**:831–842. doi:10.1038/s41593-021-
956 00828-2
957
- 958 Hung LW, Neuner S, Polepalli JS, Beier KT, Wright M, Walsh JJ, Lewis EM, Luo L,
959 Deisseroth K, Dölen G, Malenka RC. 2017. Gating of social reward by oxytocin in the ventral
960 tegmental area. *Science* **357**:1406–1411. doi:10.1126/science.aan4994

- 961
962 Inagaki TK, Muscatell KA, Moieni M, Dutcher JM, Jevtic I, Irwin MR, Eisenberger NI. 2016.
963 Yearning for connection? Loneliness is associated with increased ventral striatum activity to
964 close others. *Soc Cogn Affect Neurosci* **11**:1096–1101. doi:10.1093/scan/nsv076
965
966 Jürgens U. 1994. The role of the periaqueductal grey in vocal behaviour. *Behav Brain Res*
967 **62**:107–117. doi:10.1016/0166-4328(94)90017-5
968
969 Karigo T, Kennedy A, Yang B, Liu M, Tai D, Wahle IA, Anderson DJ. 2021. Distinct
970 hypothalamic control of same- and opposite-sex mounting behaviour in mice. *Nature*
971 **589**:258–263. doi:10.1038/s41586-020-2995-0
972
973 Killgore WDS, Cloonan SA, Taylor EC, Anlap I, Dailey NS. 2021. Increasing aggression
974 during the COVID-19 lockdowns. *J Affect Disord Rep* **5**:100163.
975 doi:10.1016/j.jadr.2021.100163
976
977 Kohl J, Babayan BM, Rubinstein ND, Autry AE, Marin-Rodriguez B, Kapoor V, Miyamishi K,
978 Zweifel LS, Luo L, Uchida N, Dulac C. 2018. Functional circuit architecture underlying
979 parental behaviour. *Nature* **556**:326–331. doi:10.1038/s41586-018-0027-0
980
981 Lee CR, Chen A, Tye KM. 2021. The neural circuitry of social homeostasis: Consequences
982 of acute versus chronic social isolation. *Cell* **184**:1500–1516. doi:10.1016/j.cell.2021.02.028
983
984 Lee H, Kim D-W, Remedios R, Anthony TE, Chang A, Madisen L, Zeng H, Anderson DJ.
985 2014. Scalable control of mounting and attack by Esr1+ neurons in the ventromedial
986 hypothalamus. *Nature* **509**:627–632. doi:10.1038/nature13169
987
988 Liu D, Rahman M, Johnson A, Tsutsui-Kimura I, Pena N, Talay M, Logeman BL, Finkbeiner
989 S, Choi S, Capo-Battaglia A, Abdus-Saboor I, Ginty DD, Uchida N, Watabe-Uchida M, Dulac
990 C. 2023. A Hypothalamic Circuit Underlying the Dynamic Control of Social Homeostasis.
991 Preprint at bioRxiv. doi:10.1101/2023.05.19.540391
992
993 Liu M, Kim D-W, Zeng H, Anderson DJ. 2022. Make war not love: The neural substrate
994 underlying a state-dependent switch in female social behavior. *Neuron* **110**:841-856.e6.
995 doi:10.1016/j.neuron.2021.12.002
996
997 Love TM. 2014. Oxytocin, motivation and the role of dopamine. *Pharmacol Biochem Behav*
998 **119**:49–60. doi:10.1016/j.pbb.2013.06.011
999
1000 Ma X, Jiang D, Jiang W, Wang F, Jia M, Wu J, Hashimoto K, Dang Y, Gao C. 2011. Social
1001 isolation-induced aggression potentiates anxiety and depressive-like behavior in male mice
1002 subjected to unpredictable chronic mild stress. *PLoS One* **6**:e20955.
1003 doi:10.1371/journal.pone.0020955
1004
1005 Ma Y-K, Zeng P-Y, Chu Y-H, Lee C-L, Cheng C-C, Chen C-H, Su Y-S, Lin K-T, Kuo T-H.
1006 2022. Lack of social touch alters anxiety-like and social behaviors in male mice. *Stress*
1007 **25**:134–144. doi:10.1080/10253890.2022.2047174
1008
1009 Machimbarrena JM, Álvarez-Bardón A, León-Mejía A, Gutiérrez-Ortega M, Casadiego-
1010 Cabrales A, González-Cabrera J. 2019. Loneliness and Personality Profiles Involved in
1011 Bullying Victimization and Aggressive Behavior. *School Ment Health* **11**:807–818.
1012 doi:10.1007/s12310-019-09328-y
1013

- 1014 Matsumoto K, Pinna G, Puia G, Guidotti A, Costa E. 2005. Social isolation stress-induced
1015 aggression in mice: a model to study the pharmacology of neurosteroidogenesis. *Stress*
1016 **8**:85–93. doi:10.1080/10253890500159022
1017
- 1018 Matthews GA, Nieh EH, Vander Weele CM, Halbert SA, Pradhan RV, Yosafat AS, Glober
1019 GF, Izadmehr EM, Thomas RE, Lacy GD, Wildes CP, Ungless MA, Tye KM. 2016. Dorsal
1020 Raphe Dopamine Neurons Represent the Experience of Social Isolation. *Cell* **164**:617–631.
1021 doi:10.1016/j.cell.2015.12.040
1022
- 1023 McHenry JA, Otis JM, Rossi MA, Robinson JE, Kosyk O, Miller NW, McElligott ZA, Budygin
1024 EA, Rubinow DR, Stuber GD. 2017. Hormonal gain control of a medial preoptic area social
1025 reward circuit. *Nat Neurosci* **20**:449–458. doi:10.1038/nn.4487
1026
- 1027 McWain MA, Pace RL, Nalan PA, Lester DB. 2022. Age-dependent effects of social isolation
1028 on mesolimbic dopamine release. *Exp Brain Res* **240**:2803–2815. doi:10.1007/s00221-022-
1029 06449-w
1030
- 1031 Mears DP, Bales WD. 2009. Supermax Incarceration and Recidivism. *Criminology* **47**:1131–
1032 1166. doi:10.1111/j.1745-9125.2009.00171.x
1033
- 1034 Melis MR, Sanna F, Argiolas A. 2022. Dopamine, Erectile Function and Male Sexual
1035 Behavior from the Past to the Present: A Review. *Brain Sci* **12**:826.
1036 doi:10.3390/brainsci12070826
1037
- 1038 Merari A, Ginton A. 1975. Characteristics of exaggerated sexual behavior induced by
1039 electrical stimulation of the medial preoptic area in male rats. *Brain Res* **86**:97–108.
1040 doi:10.1016/0006-8993(75)90641-1
1041
- 1042 Michael V, Goffinet J, Pearson J, Wang F, Tschida K, Mooney R. 2020. Circuit and synaptic
1043 organization of forebrain-to-midbrain pathways that promote and suppress vocalization. *Elife*
1044 **9**:e63493. doi:10.7554/eLife.63493
1045
- 1046 Musardo S, Contestabile A, Knoop M, Baud O, Bellone C. 2022. Oxytocin neurons mediate
1047 the effect of social isolation via the VTA circuits. *eLife* **11**:e73421. doi:10.7554/eLife.73421
1048
- 1049 Niesink RJ, van Ree JM. 1982. Short-term isolation increases social interactions of male
1050 rats: a parametric analysis. *Physiol Behav* **29**:819–825. doi:10.1016/0031-9384(82)90331-6
1051
- 1052 Otchy TM, Wolff SBE, Rhee JY, Pehlevan C, Kawai R, Kempf A, Gobes SMH, Ölveczky BP.
1053 2015. Acute off-target effects of neural circuit manipulations. *Nature* **528**:358–363.
1054 doi:10.1038/nature16442
1055
- 1056 Panksepp J, Beatty WW. 1980. Social deprivation and play in rats. *Behav Neural Biol*
1057 **30**:197–206. doi:10.1016/s0163-1047(80)91077-8
1058
- 1059 Reid JA, Chenneville T, Gardy SM, Baglivio MT. 2022. An Exploratory Study of COVID-19's
1060 Impact on Psychological Distress and Antisocial Behavior Among Justice-Involved Youth.
1061 *Crime Delinquency* **68**:1271–1291. doi:10.1177/00111287211054729
1062
- 1063 Resendez SL, Namboodiri VMK, Otis JM, Eckman LEH, Rodriguez-Romaguera J, Ung RL,
1064 Basiri ML, Kosyk O, Rossi MA, Dichter GS, Stuber GD. 2020. Social Stimuli Induce
1065 Activation of Oxytocin Neurons Within the Paraventricular Nucleus of the Hypothalamus to
1066 Promote Social Behavior in Male Mice. *J Neurosci* **40**:2282–2295.
1067 doi:10.1523/JNEUROSCI.1515-18.2020
1068

- 1069 Ritters LV. 2012. The role of motivation and reward neural systems in vocal communication
1070 in songbirds. *Front Neuroendocrinol* **33**:194–209. doi:10.1016/j.yfrne.2012.04.002
1071
- 1072 Ritters LV, Ball GF. 1999. Lesions to the medial preoptic area affect singing in the male
1073 European starling (*Sturnus vulgaris*). *Horm Behav* **36**:276–286. doi:10.1006/hbeh.1999.1549
1074
- 1075 Ritters LV, Eens M, Pinxten R, Duffy DL, Balthazart J, Ball GF. 2000. Seasonal changes in
1076 courtship song and the medial preoptic area in male European starlings (*Sturnus vulgaris*).
1077 *Horm Behav* **38**:250–261. doi:10.1006/hbeh.2000.1623
1078
- 1079 Robinson DL, Zitzman DL, Smith KJ, Spear LP. 2011. Fast dopamine release events in the
1080 nucleus accumbens of early adolescent rats. *Neuroscience* **176**:296–307.
1081 doi:10.1016/j.neuroscience.2010.12.016
1082
- 1083 Solié C, Girard B, Righetti B, Tapparel M, Bellone C. 2022. VTA dopamine neuron activity
1084 encodes social interaction and promotes reinforcement learning through social prediction
1085 error. *Nat Neurosci* **25**:86–97. doi:10.1038/s41593-021-00972-9
1086
- 1087 Tan T, Wang W, Liu T, Zhong P, Conrow-Graham M, Tian X, Yan Z. 2021. Neural circuits
1088 and activity dynamics underlying sex-specific effects of chronic social isolation stress. *Cell*
1089 *Rep* **34**:108874. doi:10.1016/j.celrep.2021.108874
1090
- 1091 Tang Y, Chen Z, Tao H, Li C, Zhang X, Tang A, Liu Y. 2014. Oxytocin activation of neurons
1092 in ventral tegmental area and interfascicular nucleus of mouse midbrain.
1093 *Neuropharmacology* **77**:277–284. doi:10.1016/j.neuropharm.2013.10.004
1094
- 1095 Tomova L, Wang KL, Thompson T, Matthews GA, Takahashi A, Tye KM, Saxe R. 2020.
1096 Acute social isolation evokes midbrain craving responses similar to hunger. *Nat Neurosci*
1097 **23**:1597–1605. doi:10.1038/s41593-020-00742-z
1098
- 1099 Toth M, Mikics E, Tulogdi A, Aliczki M, Haller J. 2011. Post-weaning social isolation induces
1100 abnormal forms of aggression in conjunction with increased glucocorticoid and autonomic
1101 stress responses. *Horm Behav* **60**:28–36. doi:10.1016/j.yhbeh.2011.02.003
1102
- 1103 Tschida K, Michael V, Takatoh J, Han B-X, Zhao S, Sakurai K, Mooney R, Wang F. 2019. A
1104 Specialized Neural Circuit Gates Social Vocalizations in the Mouse. *Neuron* **103**:459-472.e4.
1105 doi:10.1016/j.neuron.2019.05.025
1106
- 1107 Valzelli L. 1973. The “isolation syndrome” in mice. *Psychopharmacologia* **31**:305–320.
1108 doi:10.1007/BF00421275
1109
- 1110 Walum H, Young LJ. 2018. The neural mechanisms and circuitry of the pair bond. *Nat Rev*
1111 *Neurosci* **19**:643–654. doi:10.1038/s41583-018-0072-6
1112
- 1113 Warren MR, Clein RS, Spurrier MS, Roth ED, Neunuebel JP. 2020. Ultrashort-range, high-
1114 frequency communication by female mice shapes social interactions. *Sci Rep* **10**:2637.
1115 doi:10.1038/s41598-020-59418-0
1116
- 1117 Wei Y-C, Wang S-R, Jiao Z-L, Zhang W, Lin J-K, Li X-Y, Li S-S, Zhang X, Xu X-H. 2018.
1118 Medial preoptic area in mice is capable of mediating sexually dimorphic behaviors
1119 regardless of gender. *Nat Commun* **9**:279. doi:10.1038/s41467-017-02648-0
1120
- 1121 Weiss IC, Pryce CR, Jongen-Rêlo AL, Nanz-Bahr NI, Feldon J. 2004. Effect of social
1122 isolation on stress-related behavioural and neuroendocrine state in the rat. *Behav Brain Res*
1123 **152**:279–295. doi:10.1016/j.bbr.2003.10.015

- 1124
1125 Wiberg GS, Grice HC. 1963. Long-term isolation stress in rats. *Science* **142**:507.
1126 doi:10.1126/science.142.3591.507
1127
1128 Wu YE, Dang J, Kingsbury L, Zhang M, Sun F, Hu RK, Hong W. 2021. Neural control of
1129 affiliative touch in prosocial interaction. *Nature* **599**:262–267. doi:10.1038/s41586-021-
1130 03962-w
1131
1132 Xiao L, Priest MF, Nasenbeny J, Lu T, Kozorovitskiy Y. 2017. Biased Oxytocinergic
1133 Modulation of Midbrain Dopamine Systems. *Neuron* **95**:368-384.e5.
1134 doi:10.1016/j.neuron.2017.06.003
1135
1136 Yorgason JT, Calipari ES, Ferris MJ, Karkhanis AN, Fordahl SC, Weiner JL, Jones SR.
1137 2016. Social isolation rearing increases dopamine uptake and psychostimulant potency in
1138 the striatum. *Neuropharmacology* **101**:471–479. doi:10.1016/j.neuropharm.2015.10.025
1139
1140 Zelikowsky M, Hui M, Karigo T, Choe A, Yang B, Blanco MR, Beadle K, Gradinaru V,
1141 Deverman BE, Anderson DJ. 2018. The Neuropeptide Tac2 Controls a Distributed Brain
1142 State Induced by Chronic Social Isolation Stress. *Cell* **173**:1265-1279.e19.
1143 doi:10.1016/j.cell.2018.03.037
1144
1145 Zhao X, Ziobro P, Pranic NM, Chu S, Rabinovich S, Chan W, Zhao J, Kornbrek C, He Z,
1146 Tschida KA. 2021. Sex- and context-dependent effects of acute isolation on vocal and non-
1147 vocal social behaviors in mice. *PLoS One* **16**:e0255640. doi:10.1371/journal.pone.0255640

Figure 1.

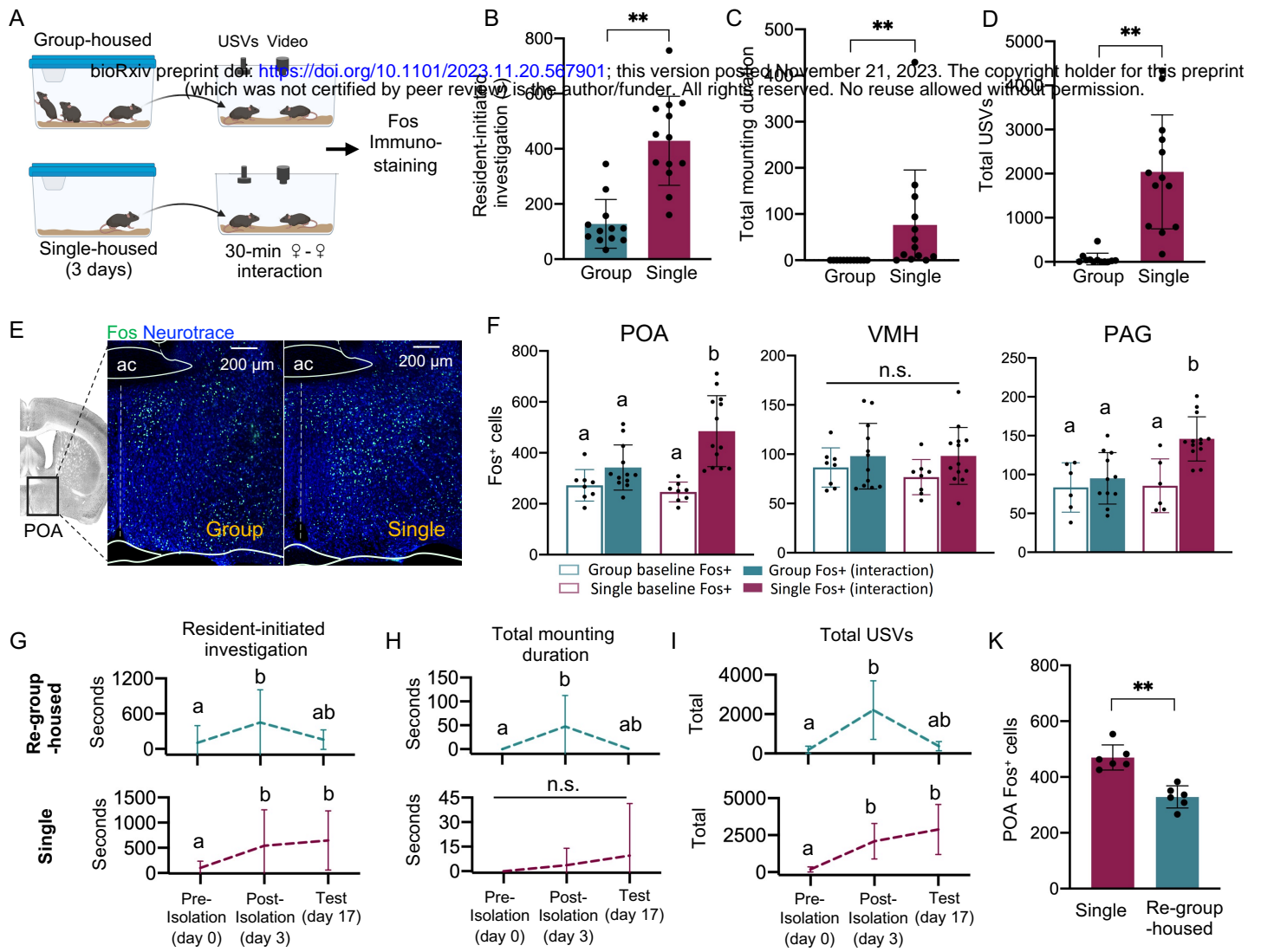
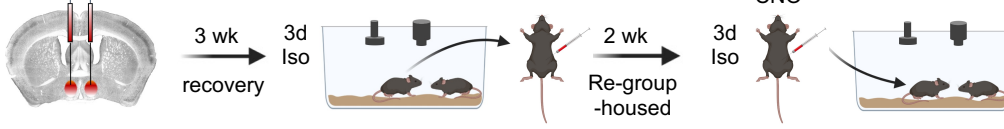


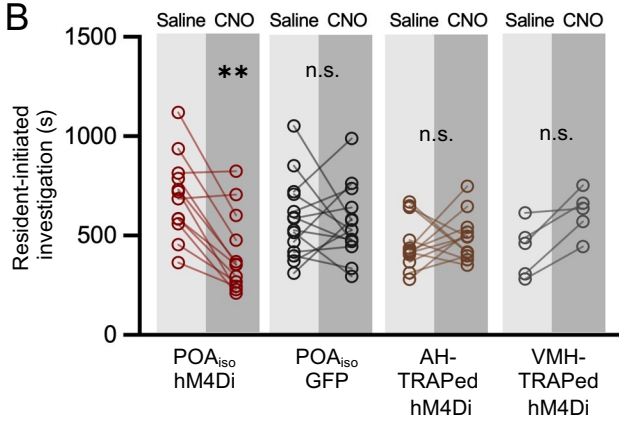
Figure 2.

A

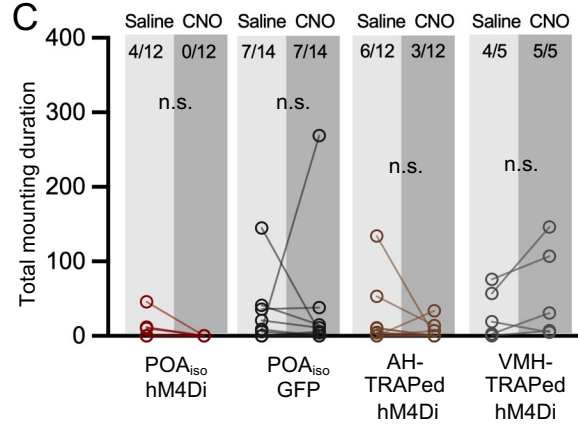
bioRxiv preprint doi: <https://doi.org/10.1101/2023.11.20.567901>; this version posted November 21, 2023. The copyright holder for this preprint (which was not certified by peer review) is the author/funder. All rights reserved. No reuse allowed without permission.



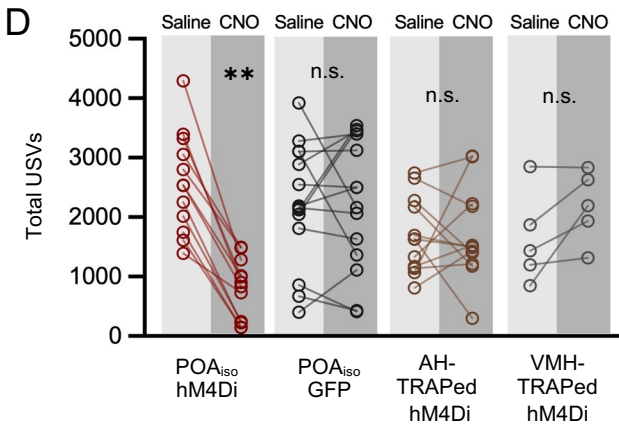
B



C



D



E

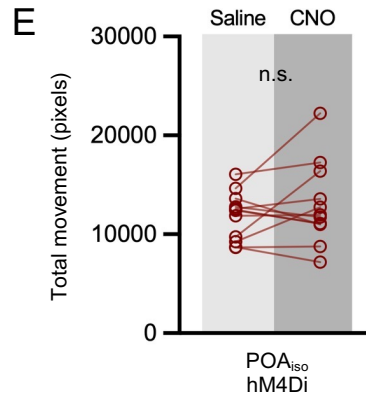
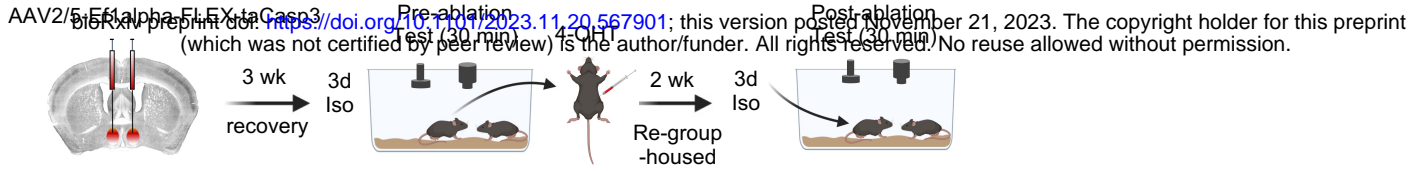
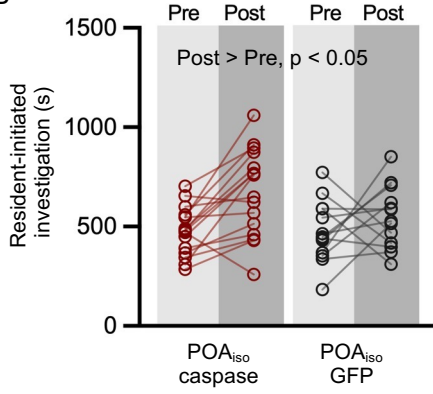


Figure 3.

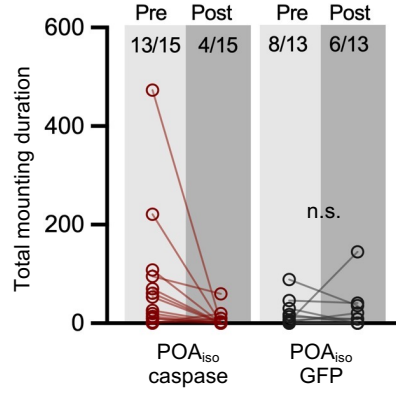
A



B



C



D

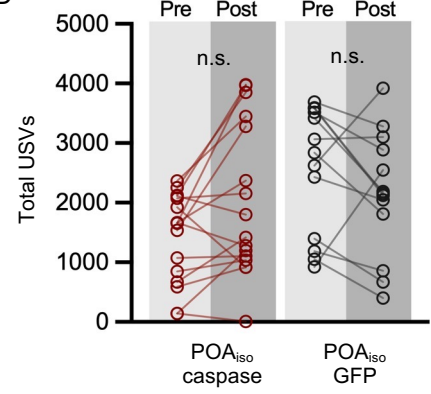


Figure 4

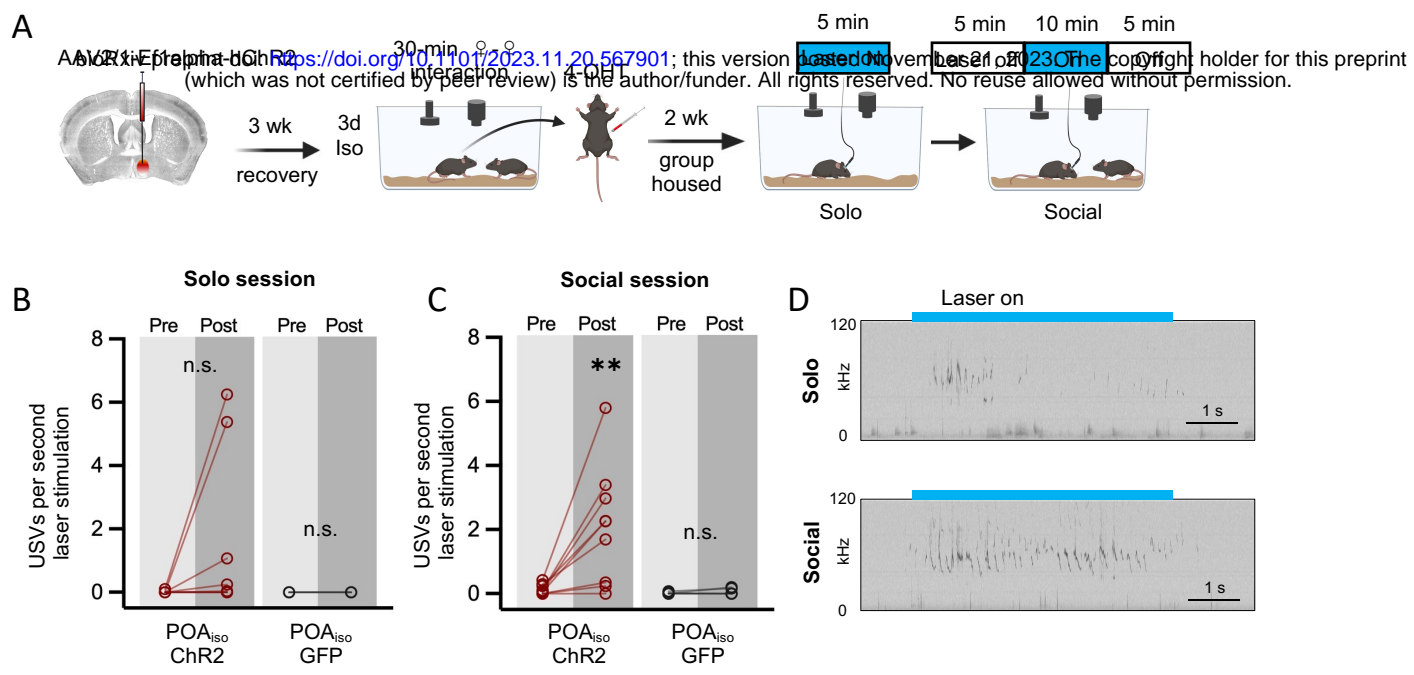


Figure 5.

